[Theses and Dissertations](#)   [Student Research](#)

2-1-2015

Channel estimation and tracking algorithms for vehicle to vehicle communications

Moustafa Awad

Follow this and additional works at: https://fount.aucegypt.edu/etds

THE AMERICAN UNIVERSITY IN CAIRO

MASTER THESIS

Channel Estimation and Tracking Algorithms for Vehicle to Vehicle Communications

Supervisor:

Dr.Karim Seddik

Author:

Moustafa Medhat Awad

Co-supervisor:

Dr.Ayman Elezabi

*A thesis submitted in partial fulfillment of the requirements
for the degree of Master of Science*

in the

Electronics and Communications Engineering

July 2015

Abstract

The vehicle-to-vehicle (V2V) communications channels are highly time-varying, making reliable communication difficult. This problem is particularly challenging because the standard of the V2V communications (IEEE 802.11p standard) is based on the WLAN IEEE 802.11a standard, which was designed for indoor, relatively stationary channels; so the IEEE 802.11p standard is not customized for outdoor, highly mobile non-stationary channels.

In this thesis,We propose Channel estimation and tracking algorithms that are suitable for highly-time varying channels. The proposed algorithms utilize the finite alphabet property of the transmitted symbol, time domain truncation, decision-directed as well as pilot information. The proposed algorithms improve the overall system performance in terms of bit error rates, enabling the system to achieve higher data rates and larger packet lengths at high relative velocities. Simulation results show that the proposed algorithms achieve improved performance for all the V2V channel models with different velocities, and for different modulation schemes and packet sizes as compared to the conventional least squares and other previously proposed channel estimation techniques for V2V channels.

Acknowledgements

All praise is due to Allah (God).

I would like to express my gratitude towards my supervisor Dr.Karim Seddik. His way of thinking, fruitful contribution, support and understanding had made my M.Sc journey more beneficial and much easier. Also i would like to thank Dr.Ayman Elezabi for his guidance through out my graduate studies.

I thank my parents so much for their support and for always pushing me forward that makes me has no choice other than to succeed. I would like to confess that without their support, i would never have been able to achieve so much. I especially want to thank my wife for being by my side and making me more confident and motivated to pursue my master's degree.

I am extremely grateful to General Nabil Elmohandes, for his support during my military service and making me able to pursue my studies.

Contents

List of Figures

List of Tables

Abbreviations

AWGN	**A**dditive **W**hite **G**aussian Noise
BER	**B**it **E**rror **R**ate
BPSK	**B**inary **P**hase **S**hift **K**eying
CDP	**C**onstructed **D**ata **P**ilots
DD	**D**ecision **D**irected
DDT	**D**ecision **D**irected **T**racking
DSRC	**D**edicated **S**hort **R**ange Communications
FA	**F**inite **A**lphabet
FDMA	**F**requency **D**ivision **M**ultiple **A**ccess
FEC	**F**orward **E**rror **C**orrection
FFT	**F**ast **F**ourier **T**ransform
IFFT	**I**nverse **F**ast **F**ourier **T**ransform
LOS	**L**ine **O**f **S**ight
LS	**L**east **S**quares
MCM	**M**ulti **C**arrier Modulation
MD	**M**inimum **D**istance
MMSE	**M**inimum **M**ean **S**quare
OFDM	**O**rthogonal **F**requency **D**ivision Multiplexing
PER	**P**acket **E**rror **R**ate
QAM	**Q**uadrature **A**mplitude Modulation
QPSK	**Q**uadrature **P**hase **S**hift **K**eying
RTV	**R**oadside **T**o **V**ehicle
STA	**S**pectral **T**emporal **A**veraging
TT	**T**ime **T**runcation
V2V	**V**ehicle **T**wo **V**ehicle

VII	**I**nfra-structure **I**ntegration **I**nitiative
WAVE	**W**ireless **A**ccess **V**ehicular **E**nvironments
WLAN	**W**ireless **L**ocal **A**rea **N**etwork

Symbols

F_M DFT matrix of size M

h channel impulse response

H channel frequency response

J smallest index of non zero coefficient

K subcarrier number

Q constellation size

R_{gy} cross covariance

R_{YY} auto covariance

S equalized symbols

V scaled FFT matrix

W subcarrier weight

X transmitted OFDM data symbols

X_p training sequence

Y FFT of the received OFDM data symbols

Z AWGN

α forgetting factor

β window size

γ constant used to remove the data effect

λ_m corresponding ambiguity in the channel response

$\boldsymbol{\Phi}$ J-fold convolution of the time domain perfect channel

ρ subcarrier frequency

To my parents, my beloved wife and daughter

Chapter 1

Introduction

1.1 Motivation

To realize many future applications in the vehicular communication that vary from simple safety messages and infotainment to autonomous driving, a robust network of connected vehicles is desired. Vehicle-to-vehicle (V2V) communications enable vehicles to stay connected to each other and react to any exchange of information.

V2V communication is a part of the intelligent transportation system that promises to increase road safety and take the driving experience to a next level where the driver can see far beyond what he usually used to see; drivers will be able to get safety messages and alerts of expected road hazards. Moreover V2V communication can reduce traffic jams and decrease road accidents by various applications [2] [3] such as traffic light optimal speed advisory, cooperative forward collision warning, hazardous location V2V notifications and remote wireless diagnosis. Futuristic V2V applications envision autonomous driving where the driver's role is just to enjoy the smooth ride.

In order to take advantage of all these upcoming applications, a robust way of communication between vehicles must be established. Accurate and reliable channel estimation is critical to the overall system performance, and in V2V communications the main challenge to system performance is the extremely time varying channel characteristics due to vehicular high speeds and the high mobility of the environment around including scatterers.

Although the fourth generation standard of mobile cellular networks can support high speeds, vehicular networks are a different story as it has two major challenges rather than only speed. First safety applications cannot withstand high delay coming from the round trip of the fourth generation (from the mobile to the base station and vice versa).

Second even non safety applications need fast connection setup with the base station because of the small time the car takes within the coverage area of a certain base station. Also the V2V environment is much more challenging than the cellular environment as both the transmitter and the receiver are moving as well as the scatterers.

The IEEE 802.11p standard (referred to as Dedicated Short Range Communication (DSRC)) is the officially implemented standard for the V2V communications. DSRC is a variant of the well-known standard IEEE 802.11a with few changes such as bandwidth and operating frequency. 802.11a is the WLAN standard which was developed for relatively stationary environment applicable for the indoor use. That is why trying to enhance the system performance while complying with the 802.11p standard is very challenging in the highly dynamic V2V channels.

The DSRC system is one of the fundamental building blocks of the US Department of Transportations' vehicle infra-structure integration (VII) initiative. VII envisions a nation-wide system in which intelligent vehicles communicate with each other and the transportation infra-structure. The purpose is to provide new services that ensure significant safety, mobility and commercial benefits. In many ways, the deployment of VII could reduce highway fatalities and improve the quality of life.

1.2 Literature Review

The majority of work done in channel estimation algorithms for OFDM systems in highly dynamic environments is independent of any specific standard while some work has been done on the channel estimation and tracking for the IEEE 802.11p standard, but the performance did not reach yet the satisfactory levels able to realize V2V critical applications.

The performance study in [4] indicated that conventional channel estimation is not a suitable choice for DSRC applications. In order to improve the performance of DSRC systems, it is necessary to track the rapid fluctuation of the channel response within the packet duration.

In [5], several equalization schemes were developed to closely track the V2V channel and thus decrease the packet error rate (PER). Through a set of empirical experiments, it was shown that the PER could be decreased using the spectral temporal averaging (STA) instead of the conventional least square estimator (LS). However, this scheme depends on the knowledge of radio environment that is hard to obtain in practice so fixed values are used instead which degrades the performance.

Also in [6], a dynamic equalization scheme was described that decreases the PER from one vehicle to another. A hardware implementation of this scheme was described to illustrate its implementation feasibility. This improved equalization was extended to all of the data rates available in the standard and showed how PER and throughput depend on packet length, payload size, and data rate. The complexity of this scheme is considerably high as decision directed channel estimation is carried out depending on the feedback from the viterbi decoder then it goes all the way back through convolutional encoder, bit interleaver, modulation and pilot insertion until a channel estimate could be made.

In [7], an advanced receiver scheme was proposed that uses decision directed channel estimation complemented with channel smoothing to reach satisfactory performance at the expense of huge increase in computational complexity due to multiplication of large matrices and also the proposed complexity reduction techniques cause performance degradation.

A survey on IEEE 802.11p current channel estimation and tracking algorithms is presented in [8], and a novel channel estimation algorithm, that outperforms the previously proposed schemes, as this scheme exploits data symbols to construct pilots and channel correlation between successive symbols. On the other hand more improvements and performance gains could be achieved as explained below.

In [9], techniques to improve the accuracy of the initial channel estimates were presented. However, this techniques are suitable only for WLAN stationary environments as the V2V short coherence time cancels out any improvement achieved in the initial channel estimates and a tracking algorithm is needed to update the initial channel estimates to be able to track the channel variations.

In [10], channel estimation and tracking is done using decision directed feedback by decoding the data symbols and re-modulating them in order to get channel estimates throughout the packet duration. Viterbi decoding and re-modulation of OFDM symbols make the application of this technique costly.

In [11], vehicle speed, signal to noise ratio and packet length are exploited to closely track the channel variations using data symbols.

On the other hand, in [12] a design of a more efficient physical layer is presented using time domain differential OFDM. Although this technique is suitable for mobile environments, it requires changes in the IEEE 802.11p standard.

1.3   IEEE 802.11p Vs IEEE 802.11a

DSRC physical layer (IEEE 802.11p) [13] was originally adopted from IEEE 802.11a [14] standard, which uses an OFDM physical layer. Through the use of a guard interval, OFDM can mitigate intersymbol interference due to multipath fading. However, IEEE 802.11a was designed for stationary indoor environments with low delay spread. Wireless access vehicular environments (WAVE) involve dense urban centers, which tend to have high delay spreads that would exceed the length of the guard time in IEEE 802.11a. For this reason, the symbol duration was doubled, and so, inherently, the guard time was also doubled from 0.8 to 1.6ms. Because 802.11p is a packet-based transmission, channel estimation is done by transmitting known training symbols at the beginning of each packet. The channel is estimated only once for each packet and is used to equalize the whole packet. Because of the time varying channel nature, coupled with the fact that the 802.11p standard does not limit the packet length, the channel estimate performed for each packet can be quickly outdated. In addition, the 802.11p standard only uses four pilot subcarriers in each OFDM symbol. These pilot subcarriers are not spaced close enough to reflect channel variation in the frequency domain. Therefore, the main challenge is to identify an accurate way for updating the channel estimate over the entire packet length while sticking to the standard.

The major drawback of IEEE 802.11a is that it was designed for stationary environments. Conventional IEEE 802.11a receivers initially estimate the channel response

Parameters	IEEE 802.11a	IEEE 802.11p half clocked mode	Changes
Bit rate (Mbit/s)	6, 9, 12, 18, 24, 36, 48, 54	3, 4.5, 6, 9, 12, 18, 24, 27	Half
Modulation mode	BPSK, QPSK, 16QAM, 64QAM	BPSK, QPSK, 16QAM, 64QAM	No change
Code rate	1/2, 2/3, 3/4	1/2, 2/3, 3/4	No change
Number of subcarriers	52	52	No change
Symbol duration	4 µs	8 µs	Double
Guard time	0.8 µs	1.6 µs	Double
FFT period	3.2 µs	6.4 µs	Double
Preamble duration	16 µs	32 µs	Double
Subcarrier spacing	0.3125 MHz	0.15625 MHz	Half

TABLE 1.1: Physical layer implementations Comparison [1] in IEEE 802.11a and IEEE 802.11p.

based on a known preamble in the packet header. The channel response is assumed to be relatively static for the entire packet duration; therefore, the entire packet is compensated based on the initial channel estimate. On the other hand, V2V communications have a small coherence time and a narrow coherence bandwidth due to the fact that the transmitter, receiver and the scatterers are all in motion. Due to these characteristics, channel estimation is not an easy job as the channel varies vastly during the same packet duration.

IEEE 802.11a usually uses the full clocked mode with 20 MHz bandwidth, while IEEE 802.11p usually uses the half clocked mode with 10 MHz bandwidth. And this implies the 802.11p signal more robust against fading, the carrier spacing is reduced by half and the symbol length is doubled. In addition to that the IEEE 802.11p operates in the 5.9 GHz frequency bands.

1.4   Thesis Contribution

In this thesis, we propose three different channel estimation and tracking algorithms tailored to deal with the pilot structure of the 802.11p standard as well as V2V channel characteristics. In the first algorithm, we implement a semi-blind channel estimation algorithm benefiting from the finite alphabet property of the transmitted symbols. In the second algorithm, we propose to use decision directed channel estimation combined with time domain truncation to alleviate some of the effects of error propagation. In the third algorithm, the pilot information and the high correlation characteristic of the channel response between adjacent subcarriers are exploited to track the channel variations in a simple intuitive way leading to a low complexity algorithm that is easy to implement.

1.5   Thesis Organization

In Chapter 2, we present a background overview of the OFDM system as well as the IEEE 802.11p OFDM model, transmitter components and receiver components.

Chapter 3 presents the V2V channel characteristics, the standard channel model and the channel scenarios adopted for the simulation.

Chapter 4 constitutes the major contribution of the thesis, in which we consider the design of different channel estimation algorithms. Besides, the basic equalization scheme that is typical of IEEE 802.11a standard. Also simulation results are presented for performance comparison.

In chapter 5, we present the thesis conclusion and some directions for future research.

Chapter 2

System Model

2.1 OFDM Background

Multi-Carrier Modulation (MCM) is the main idea behind OFDM. MCM is achieved by splitting the input bit stream into different parallel bit streams to transmit the data, each of these parallel streams has lower bit rate, these sub-streams are used to modulate different carriers as shown in Fig. 2.1.

The Military radio links were the first to use MCM in the late 1950s and the early 1960. In 1966 Chang's patent introdused the main idea of OFDM which is a special form of MCM with densely spaced subcarriers and overlapping spectra. The use of steep bandpass filters was limited after the introduction of OFDM as they were used to completely separate each sub-carrier spectrum while in OFDM the sub-carriers' spectra
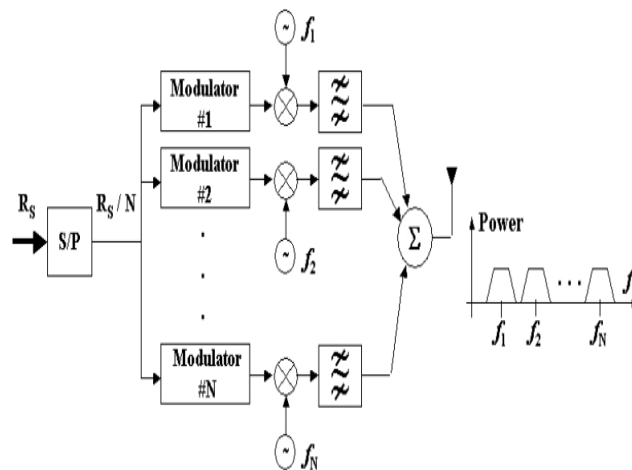
FIGURE 2.1: Block Diagram of MCM transmitter.
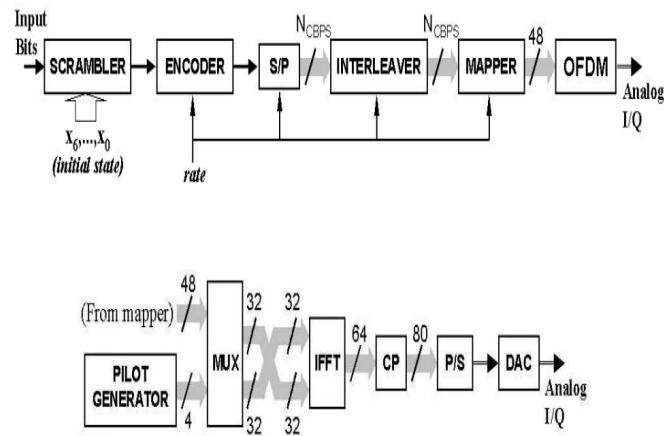
FIGURE 2.2: Baseband transmitter model.

are overlapped in contrast to conventional analogue FDMA systems. Although, carriers spectrum overlap in OFDM systems, time domain waveforms must be chosen to be mutually orthogonal. Fast Fourier transform is applied on the input stream to acheive the required orthogonality. The introduction of OFDM sytems into real systems was delayed due to implementation aspects. Powerful digital signal processors were required to meet the real time FFT complexity. Moreover, highly stable oscillators and linear power amplifiers were needed to achieve orthogonality between various subcarriers. Since the beginning of the 1990s OFDM gained a lot of interest as the many of the implementation issues became solvable [15]. The motivation behind OFDM system is the advantages when data is transmitted through a fading channel. The maximum delay spread is one of the most important parameters characterizing fading channel, and as OFDM transmitters split the input bit stream into various parallel bit streams so the symbol duraction is increased and consequently the relative delay spread will decrease.

2.1.1   IEEE 802.11p OFDM model

The IEEE 802.11p [13] and IEEE 802.11a [14] standards are working in the 5 GHz ISM as well as making use of the OFDM transmission scheme and having similar physical layers. Fig.2.2 shows the basic base-band transmitter model of both standards. The convolutional encoder, the interleaver and the mapper behaviors are determined by the rate parameter that indicates the transmission rate. Various modulation schemes and code rates are shown in table 2.1 for different rates of both standards. A brief description of various basic blocks of the OFDM transmitter is given below.

Nominal rate (Mbps)	Coding rate (Rc)	Coded bits per OFDM symbol (N_{CBPS})	Data bits per OFDM symbol (N_{DBPS})	Modulation
6	1/2	48	24	BPSK
9	3/4	48	36	BPSK
12	1/2	96	48	QPSK
18	3/4	96	72	QPSK
24	1/2	192	96	16-QAM
27[*]	9/16	192	108	16-QAM
36	3/4	192	144	16-QAM
48[**]	2/3	288	192	64-QAM
54	3/4	288	216	64-QAM

TABLE 2.1: Rate Dependant Parameters.
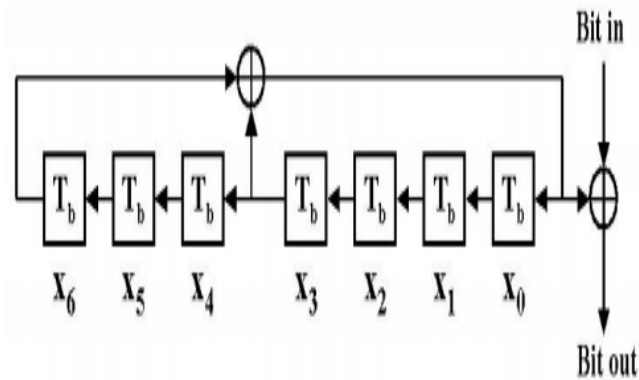
FIGURE 2.3: Scrambler Block Diagram.

Scrambler : The scrambler is mainly used to randomize the input bits, in order to achieve same bit probability at the output. Fig. 2.3 shows the scrambler's block diagram. A pseudo random generator is used to initialize the state parameters $x_0, ...x_6$ to non zero value.

Convolutional encoder : Channel coding is done firstly by the convolutional encoder. Fig. 2.4 shows it's structure. To increase system immunity against noise, correlation between several consecutive bits is introduced assuming no correlation between the bits and noise. On the receiver side, this correlation is exploited by the decoder to extract the bits from noise. Interleaver : To protect the the data against bursty channel errors, the second part of the channel coding is done at in the interleaver. In order to recover the original

FIGURE 2.4: Convolution Encoder Block Diagram.

FIGURE 2.5: Mapper Block Diagram.

bits from a noisy signal, correlation in done to consecutive bits using the convolutional encoder but if the noise hit these consecutive bits we won't be able to recover the original bits correctly. That's why the interleaver is used to transmit consecutive coded bits into non consecutive subcarriers to make the signal immune to bursty errors of the channel.

Mapper : This block is used to map the input bits to one of the following amplitude modulation schemes : BPSK, QPSK, 16-QAM, 64-QAM. The block takes a group of coded and interleaved bits to generate groups of 48 complex values as shown in Fig. 2.5.

OFDM transmission block : The transmitted information is loaded on 64 sub-carriers

enumerated $K = -32, ..., +31$, but not all of the 64 sub-carriers contain user information. There are only 48 subcarriers used for carrying data information, while 12 subcarriers are used as guard band to reduce the adjacent channel interference at positions $k = [-32, -27]union[+27, +31]$ and the middle subcarriers at position $k = 0$ is set to zero to avoid RF problems, and the remaining 4 subcarriers at the positions $K = -21, -7, +7, +21$ are used as pilots needed in some operations at the receiver side such as channel estimation as discussed later in chapter 4.

IFFT : DFT/IDFT is implemented using FFT/IFFT algorithm as the total number of subcarriers is a power of 2.

Cyclic prefix : To Compensate for the channel delay spread the last part of the signal is inserted in the beginning of the signal. The cyclic prefix duration must be larger than multipath delay spread. The orthogonality of the carriers is not affected by the cyclic prefix.

2.2 Transmitter Components

In a WAVE channel, deep fades may cause a long sequence of errors, which may render the decoder ineffective. In order to alleviate symbol correlation, the encoded bits are scrambled with a block interleaver. The length of the block interleaver corresponds to one OFDM data symbol. The dimension of the block depends on the modulation scheme selected. The available digital modulation schemes include the Gray-coded constellations of binary phase-shift keying (BPSK), QPSK, 16-QAM and 64-QAM. The interleaved bits are digitally modulated and divided into 48 sub-channels with four fixed pilot tones. The parallel data are then multiplexed into a 64-point inverse fast fourier transform (IFFT). The output of IFFT, is then converted to high speed serial data. Finally, the cyclic prefix is added.

2.3 Receiver Components

At the receiver, shown in Fig. 2.7, the cyclic prefix is removed from the received signal. The parallel data are demultiplexed into the FFT, yielding the following output in the frequency domain

$$Y_n(k) = H_n(k)S_n(k) + Z_n(k), \qquad (2.1)$$

where $Y(k)$ and $S(k)$ denote the FFT of the received and transmitted OFDM data symbols, respectively, n represents the symbol index, k represents the subcarrier number,
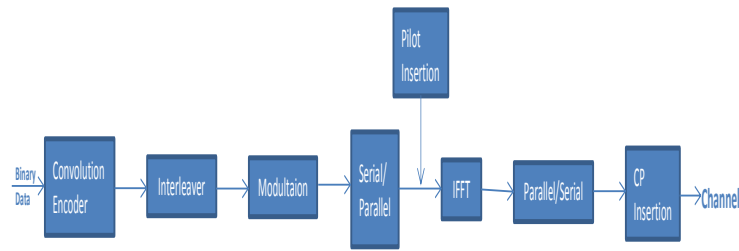
FIGURE 2.6: IEEE 802.11p Transmitter Components.
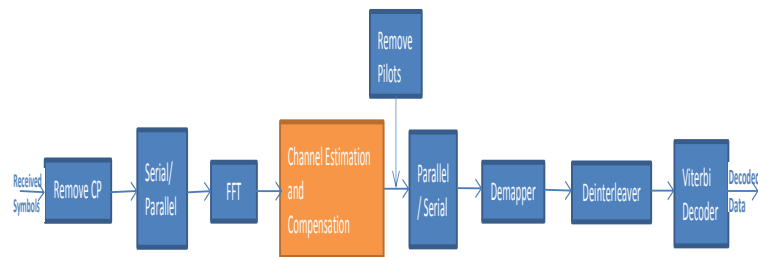
FIGURE 2.7: IEEE 802.11p Receiver Components.

$H_n(k)$ represents the channel response and $Z_n(k)$ represents the additive white Gaussian noise (AWGN). After demultiplexing, the data are compensated, digitally demodulated, deinterleaved and finally decoded using the Viterbi algorithm.

Conventional IEEE 802.11 systems assume that the channel has time-invariant fading, which means that the channel response remains constant for the entire packet duration. Hence the following assumption is made; at the signal compensator, all of subsequently received data symbols of the packet are compensated by the initial estimated channel response. A conventional WLAN system receiver cannot be applied to vehicular environments, so the receiver has to be modified to incorporate an accurate channel tracking technique. The design modifications will be limited to the receiver alone.

Chapter 3

V2V Channel Modeling

3.1 Introduction

Knowledge of the V2V propagation channel is essential for the design and performance evaluation of the whole V2V system. In the past, most of the research efforts were directed towards studying the channel characterization between a static base station and a mobile device as the case of cellular communication systems. As deep understanding of the vehicular channel characterization is of a great importance for simulation and performance enhancements, V2V channel measurement campaigns were conducted in a different environments for the possible V2V scenarios and it turned out that the V2V channel is absolutely different from the popular cellular channels in terms of both frequency and time selectivity as well as the fading statistics.

In 2006 when the IEEE 802.11p standard, which is a part of the Wireless Access in Vehicular Environments (WAVE), was published, a lot of research interest all over the world was directed towards studying the V2V channels as well as different channel models were derived based on various measurement campaigns. V2V channel modeling efforts could be found in [16], [17], [18], [19], [20]. In this thesis, the channel model proposed in [21] [22] is the adopted channel model.

3.2 Propagation Characteristics of Mobile Radio Channels [23]

In an ideal radio channel, the received signal would consist of only a single direct path signal, which would be a perfect reconstruction of the transmitted signal. However, in a real channel the signal is modified during transmission. The received signal consists of a

13

combination of attenuated, reflected, refracted, and diffracted replicas of the transmitted signal. On top of all this, the channel adds noise to the signal and can cause a shift in the carrier frequency if either of the transmitter or receiver is moving (Doppler Effect). Understanding of these effects on the signal is important because the performance of a radio system is dependent on the radio channel characteristics.

3.2.1 Attenuation

Attenuation is the drop in the signal power when transmitting from one point to another. It can be caused by the transmission path length, obstructions in the signal path, and multipath effects. Any objects which obstruct the line of sight of the signal from the transmitter to the receiver, can cause attenuation. Shadowing of the signal can occur whenever there is an obstruction between the transmitter and receiver. It is generally caused by buildings and hills, and is the most important environmental attenuation factor. Shadowing is the most severe in heavily built up areas, due to the shadowing from buildings. However, hills can cause a large problem due to the large shadow they produce. Radio signals diffract off the boundaries of obstructions, thus preventing total shadowing of the signals behind hills and buildings. However, the amount of diffraction is dependent on the radio frequency used, with high frequencies scatter more than low frequency signals. Thus high frequency signals, especially, Ultra High Frequencies (UHF) and microwave signals require line of sight for adequate signal strength, because these scatter too much. To overcome the problem of shadowing, transmitters are usually elevated as high as possible to minimize the number of obstructions.

3.2.2 Multipath Effects

3.2.2.1 Rayleigh Fading

In a radio link, the RF signal from the transmitter may be reflected from objects such as hills, buildings, or vehicles. This gives rise to multiple transmission paths at the receiver. The relative phase of multiple reflected signals can cause constructive or destructive interference at the receiver. This is experienced over very short distances (typically at half wavelength distances), which is given the term fast fading. These variations can vary from 10-30dB over a short distance. The Rayleigh distribution is commonly used to describe the statistical time varying nature of the received signal power. It describes the probability of the signal level being received due to fading.

3.2.2.2   Frequency Selective Fading

In any radio transmission, the channel spectral response is not flat. It has dips or fades in the response due to reflections causing cancellation of certain frequencies at the receiver. Reflections off near-by objects (e.g. ground, buildings, trees, etc) can lead to multipath signals of similar signal power as the direct signal. This can result in deep nulls in the received signal power due to destructive interference. For narrow bandwidth transmissions if the null in the frequency response occurs at the transmission frequency then the entire signal can be lost. This can be partly overcome in two ways. By transmitting a wide bandwidth signal or spread spectrum as in the case of CDMA, any dips in the spectrum only result in a small loss of signal power, rather than a complete loss. Another method is to split the transmission up into many carriers carrying low rate data, as is done in a COFDM/OFDM

3.2.2.3   Delay Spread

The received radio signal from a transmitter consists of typically a direct signal plus signals reflected off object such as buildings, mountains, and other structures. The reflected signals arrive at a later time than the direct signal because of the extra path length, giving rise to a slightly different arrival time of the transmitted pulse. The signal energy confined to a narrow pulse is spreading over a longer time. Delay spread is a measure of how the signal power is spread over the time between the arrival of the first and last multipath signal seen by the receiver. In a digital system, the delay spread can lead to inter-symbol interference. This is due to the delayed multipath signal overlapping symbols that follows. This can cause significant errors in high bit rate systems, especially when using time division multiplexing (TDMA). As the transmitted bit rate is increased the amount inter symbol interference also increases. The effect starts to become very significant when the delay spread is greater then 50% of the bit time.

3.3   V2V Channel Uniqueness

There are fundamental reasons for which the vehicular channel is totally different from the cellular channel and the indoor channel. First, both the transmitter, the receiver as well as the scatterers are moving so this implies wide delay spread and fast varying channel impulse response. Second, the transmitting and the receiving antennas are at the same height which implies that scattering can occur at the transmitter side and the receiver side as well, and the propagation lies on the horizontal plane within a short communications range (less than 100 m). Third, the vehicular channel suffers from

long delay spread if compared with the indoor channel which may cause inter symbol interference. Fourth, the frequency operation range of vehicular communications is 5.9 GHz so the signal suffers from higher path loss than cellular systems operating at 700-2100 MHz.

3.4 V2V Channel Characterization

V2V channel characteristics are investigated in [24] - [33]. In a wireless channel, signal propagation from the transmitter to the receiver can take several paths and each path suffers from several reflections, diffractions and attenuation. At the receiver side, the different attenuated, delayed and phase shifted versions of the transmitted signal are added up to compose the received signal. The channel impulse response is interpreted as the superposition of all the multipath components. Due to the motion of the transmitter, the receiver and the scatterers the V2V channel characteristics are time varying as well as the channel impulse response. So in order to have a reliable channel model we have to work with a large sequence of channel impulse responses which is not an easy task to do. That is why several statistical channel metrics were derived to represent a compact channel characterization. Path loss, fading statistics, delay spread and Doppler spread are the main statistical channel metrics.

TABLE 3.1: 802.11p standard channel models

Scenario	Distance between the Tx & Rx (m)	Velocity (Km/hr)	Doppler Shift (Hz)	Excess Delay (μS)
V2V Expressway Oncoming	300-400	104	1000-1200	0.3
V2V Urban Canyon Oncoming	100	32-48	400-500	0.4
RTV Suburban Street	100	32-48	300-500	0.7
RTV Expressway	300-400	104	600-700	0.4
V2V Expressway same direction with wall	300-400	104	900-1150	0.7
RTV Urban Canyon	100	32-48	300	0.5

3.4.1 Scenario Description

3.4.1.1 V2V Expressway Oncoming

Two vehicles moving with speed 65 mi/h in a highway without a middle wall

3.4.1.2 V2V Urban Canyon Oncoming

Two vehicles moving with speed 20-30 mi/h in a dense traffic area.

3.4.1.3 RTV Suburban Street

A 6.1 meter high antenna placed near an intersection with target range of 100 m. The receiver vehicle moving at speed 20-30 mi/h in the antenna range from the four possible directions.

3.4.1.4 RTV Expressway

A half dome 6.1 meter high antenna placed off a side of a expressway with target range of 100 m. The receiver vehicle moving at speed 65 mi/h approaching the antenna from the both directions of the expressway.

3.4.1.5 V2V Expressway

Two vehicles moving with speed 65 mi/h in a highway with 300-400 m separation and a middle wall between oncoming lanes

3.4.1.6 RTV Urban Canyon

A 6.1 meter high antenna placed near an urban intersection with target range of 100 m. The receiver vehicle moving at speed 20-30 mi/h in the antenna range.

3.4.2 Simulated Channel model

In our simulations, we adopted the standard 802.11p channel models in [34], where six channel models are defined for different vehicular scenarios as shown in Table 3.1 and the type of model we consider is the tapped-delay line, where each tap process is described

as by a Doppler power spectral density (PSD) having Rayleigh fading and the channel impulse response has 8 taps.

Chapter 4

Channel Estimation

4.1 Channel Estimation Fundamentals

Channel state information is the channel properties of the communication link that describe how the signal propagates from the transmitter to the receiver as it suffers from scattering, fading and power decay. Knowing this kind of information is a must at the receiver side in order to compensate for these channel effects and be able to extract the transmitted data.

Channel estimation and tracking is crucial for achieving reliable communication as channel conditions vary and instantaneous channel estimates are needed to track these variations.

The channel effects are like a filter. Channel estimation is to estimate the filter coefficient through received signal and other known information (such as modulation type and channel characteristics)

There are two approaches of designing the channel estimation module for the IEEE 802.11p standard. First approach needs structure modification of the standard as found in [35] - [37]. the second approach remain the standard structure as found in [38] - [42].

Channel estimation algorithms can be classified into three categories; training-based, blind, and semi-blind algorithms [43]. For time varying channels, training-based schemes require the frequent transmission of training sequences which can result in wasting the system resources. On the other hand, blind channel estimation techniques rely on the statistical properties of the information sequences to estimate the channel coefficients. However, they are in general computationally expensive and suffer from low convergence speed. Semi-blind channel estimation techniques strike a balance between computational complexity and consuming the system resources.

19

4.2 Simulation Environment

The design and performance of conventional DSRC systems are discussed in [44], [45], [46]. Since the conventional DSRC system is not feasible for WAVE, we propose receiver modifications that enable the system to achieve acceptable performance under high velocities, high data rates and large packet lengths. DSRC physical layer was simulated using MATLAB. The BER is the performance measure of the system. In each simulation, the BER was calculated based on the transmission of 10000 packets under varying SNRs and velocities. The initial focus is to test the performance limitations under the worst case scenario, which is a fading channel with no LOS (i.e. Rayleigh fading channel), maximum doppler and packet size.

4.2.1 Simulation Parameters

The systems were simulated with varying SNR, velocity, packet lengths and modulation scheme (i.e. data rate). The focus was placed on the effects of envelope fading, since the delay spread issues were resolved by the extension of the guard interval. The simulation range of SNR was taken from 0 to 30 dB. The maximum simulated velocity was 104 km/h. The packet lengths were ranging from 10 to 200 OFDM data symbols per packet.

4.2.2 Performance of proposed designs against conventional design

A thorough comparison between the conventional least squares and the proposed designs is presented as BER plots. A plethora of results were produced; however, only few plots are presented as examples without loss of generality. The figures presented show the BER plots for BPSK, QPSK and 16 QAM, Several V2V and RTV scenarios with different OFDM symbols per packet ranging from 10 to 200 for BPSK, 50 for QPSK and 25 for 16QAM.

4.3 Block Type Pilot Channel Estimation

Under the assumption of slow fading channel, block type pilot channel estimation is done in OFDM systems by periodically inserting pilots into all subcarriers of OFDM symbols within a specific period of time. At the receiver side, channel estimation is performed using the received signals, pilots and may or may not need certain knowledge about the channel statistics. These channel estimates are used for equalization for all the up coming OFDM symbols in the same packet until another pilot symbol is received.

4.3.1 Least Squares Estimator

As a bench mark, least squares estimator is used to estimate the channel using the two similar preamble symbols sent before the data symbols at the beginning of each packet. The first two received symbols Y_{P1} and Y_{P2} are divided by the known training sequence X_P where P refers to preamble then averaged to get the channel estimate for all subcarriers given by

$$\hat{H}_{LS}(k) = \frac{Y_{P1}(k) + Y_{P2}(k)}{2X_P(k)}, \tag{4.1}$$

where $\hat{H}_{LS}(k)$ is the least squares channel estimate on the kth subcarrier. LS estimators are low complexity estimators that don't need any knowledge about the channel statistics but suffer from high mean square error. The IEEE 802.11a standard uses this estimate to compensate for the channel effects for all the upcoming data symbols in the same packet, where the channel is assumed to be constant throughout the whole packet length; this can not be a valid assumption in the case of the 802.11p as the channel varies significantly from one symbol to another due to fast varying environment dynamics specially at very high vehicular speed and even at low vehicle speed. In V2V channels, the LS estimate will be outdated after few symbols and cannot support the maximum size packets defined by the standard or even relatively large packets.

4.3.2 Minimum Mean Square Error Estimator

Using the channel second order statistics, MMSE estimators achieve the minimum mean square error. The MMSE channel estimates are derived using equations derived in [47]. Under the assumption that the channel vector h is Gaussian and uncorrelated with the channel noise z

$$G_{MMSE} = R_{hy}R_{yy}^{-1}y, \tag{4.2}$$

$$R_{hy} = E[hy^H] = R_{hh}F^H X^H, \tag{4.3}$$

$$R_{YY} = E[yy^H] = XFR_{hh}F^H X^H + \sigma^2 I_N, \tag{4.4}$$

$$H_{MMSE} = FFT(G_{MMSE}) \tag{4.5}$$

where X denotes known data S, F is the DFT matrix, R_{hy} is the cross covariance between h and y, R_{yy} is the auto-covariance of vector y and R_{hh} is the auto-covariance of vector h and σ^2 is the noise variance. From the channel model in [34],the channel has 8 taps in the time domain so R_{hh} could be formulated by inserting ones in the first 8 diagonal elements of a 64x64 zeros matrix assuming that all of the taps have the same power.

The MMSE estimator provides much better performance than the LS estimators, especially under low SNR conditions at the expense of higher computational complexity; due to matrix inversion during each execution.

4.3.3   Decision Directed Tracking (DDT)

In order to track the fast varying channel during the same block, DDT is used to improve the performance [48]. The initial channel estimate is calculated using LS or MMSE estimators, then the channel is updated for the following OFDM symbols in the same block by demodulating the symbol based on the previous channel estimate then using the demodulated symbol to get the updated channel(Decision directed will be illustrated more later in this chapter).

4.3.4 Performance Comparison

Decision directed tracking enables the algorithm to track large packets but still the performance at fast varying environments is not acceptable.

The algorithms are simulated in both stationary and vehicular environments (200 Hz and 1000 Hz maximum doppler respectively), also different packet sizes where used.

The results show that the MMSE estimator achieve the best performance in stationary environments with small packets, while it's performance decreases vastly in fast varying environments with large packets. Hence, MMSE is not suitable for vehicular communications.

FIGURE 4.1: BPSK Bit Error Rate, maximum doppler=200Hz and 10 OFDM symbol per packet.

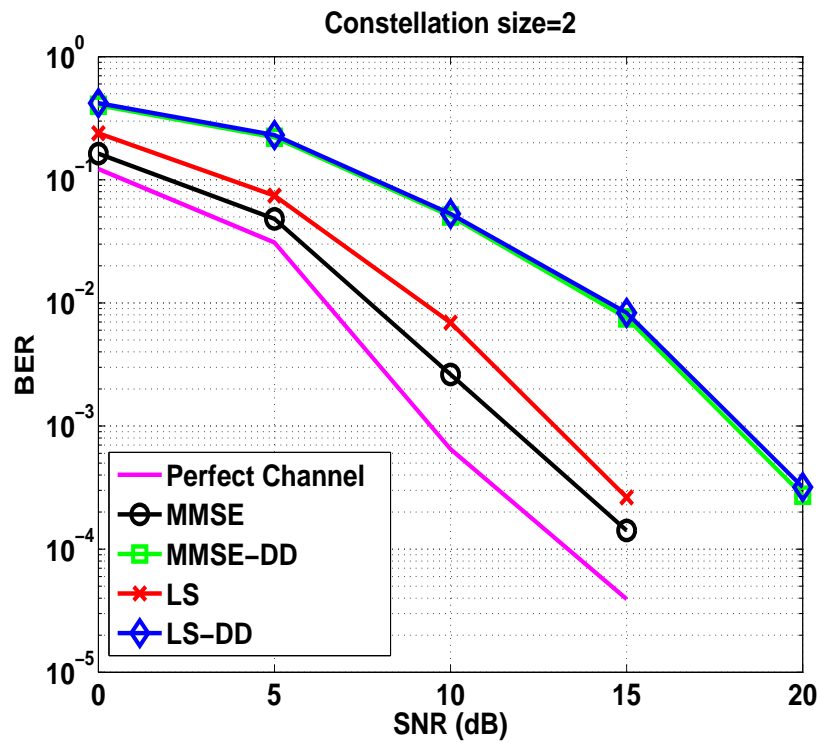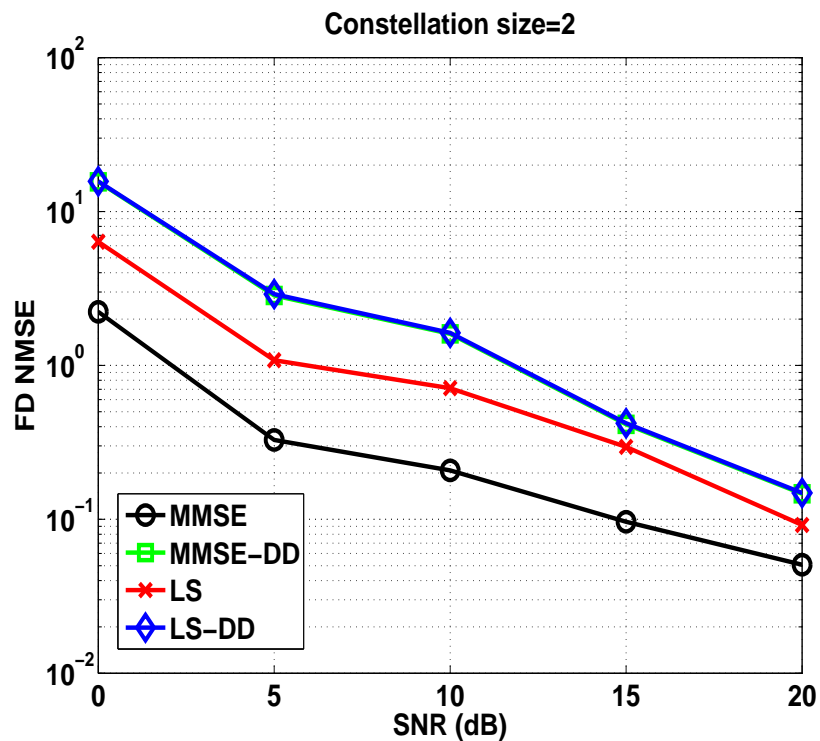FIGURE 4.2: BPSK Mean Square Error, maximum doppler=200Hz and 10 OFDM symbol per packet.
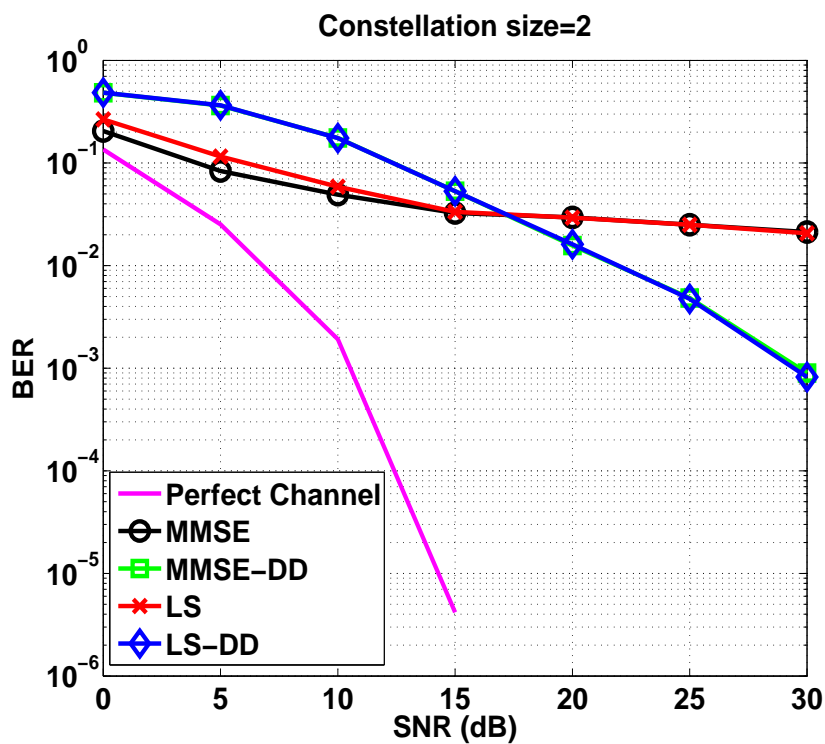

FIGURE 4.3: BPSK Bit Error Rate, maximum doppler=200Hz and 100 OFDM symbol per packet.
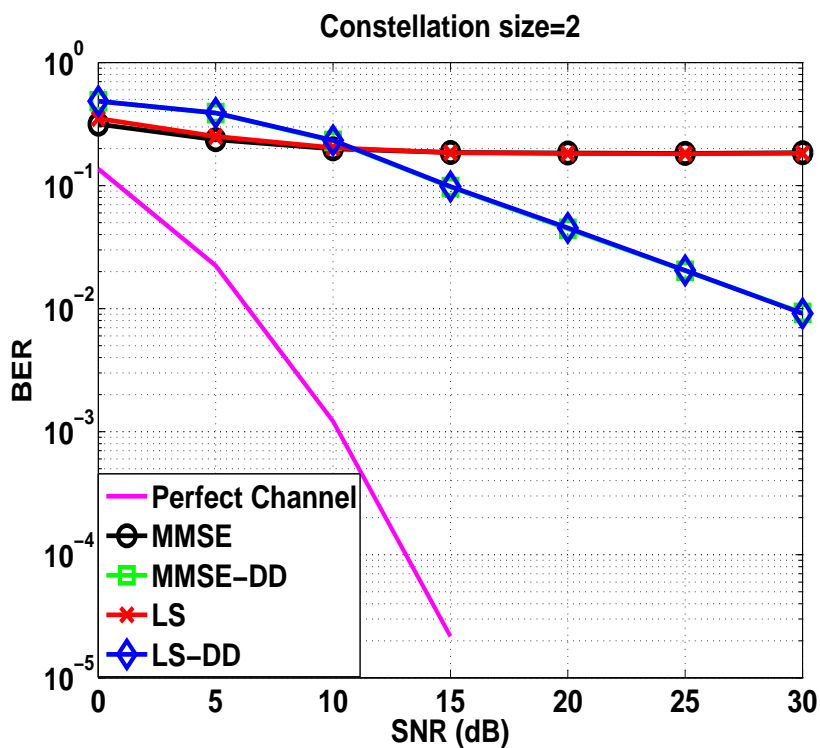
FIGURE 4.4: BPSK Bit Error Rate, maximum doppler=500Hz and 100 OFDM symbol per packet.
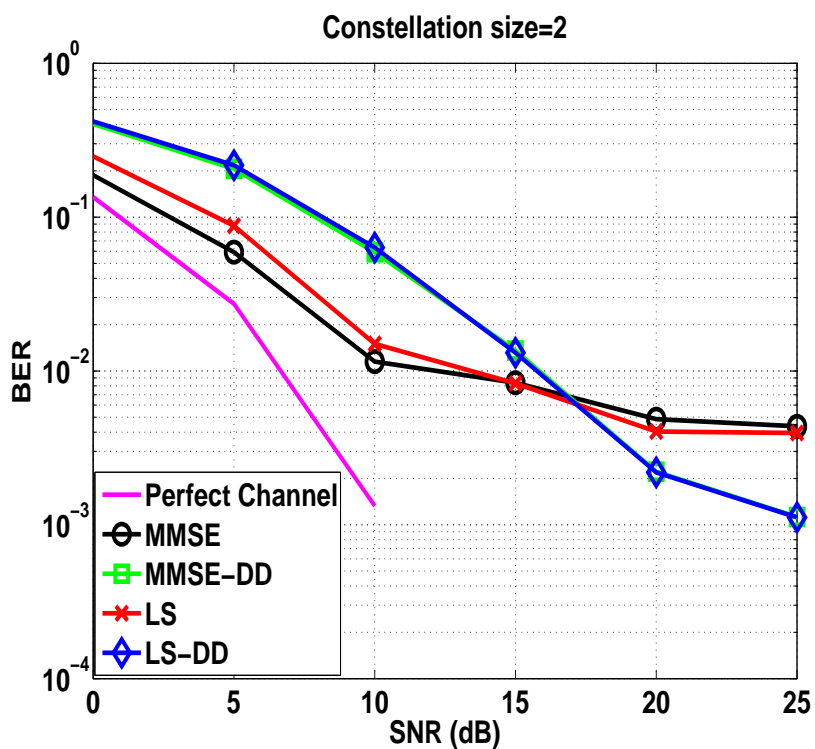

FIGURE 4.5: BPSK Bit Error Rate, maximum doppler=1000Hz and 10 OFDM symbol per packet.

4.4 Comb Type Pilot Channel Estimation

Pilots are uniformly inserted in each transmitted OFDM sysmbol but with certain sub-carriers separated from each other. Channel estimation is done by trying to estimate the channel in data subcarriers depending on the LS channel estimates of pilot subcarriers and any other channel statistics available as well as the received signals.

In order to track the channel variations in the time and frequency domains, the pilots must be spaced in a way to sample the channel fulfilling the the Nyquist criteria to be able to equalize the received signal.

The IEEE 802.11p standard uses subcarriers numbered from -26 to 26, where the zero frequency subcarrier is not used as well as unused sub carriers from -32 to -27 and from 27 to 31 which are used as a guard band. Only 4 pilots exist in the following subcarriers -21,-7,7 and 21 each OFDM symbol. The remaining 48 subcarriers are used for data transmission.

The pilots are used for frequency offset tracking. Although, the pilots are not enough to estimate the channel variations, but some information about the channel is better than nothing. Comb Type Pilot channel estimation use the information about the channel at the pilots' location to be able to update the channel estimate to track channel variations during the same OFDM symbol.

4.4.1 Pilot Interpolation Estimator

First, each received symbol is demodulated. Second,the demodulated values at pilot's positions are extracted and LS channel estimation is done on these subcarriers

$$H_p(k) = \frac{Y_p(k)}{X_p(k)}. \tag{4.6}$$

Third, the channel estimates at all other subcarriers are calculated by interpolation and it was found by experimentation that using the mean of the pilots' channel estimates at the endpoints instead of extrapolating gives more reasonable results

$$\hat{H}_p = [m_{H_p} H_P{}^T m_{H_p}]^T. \tag{4.7}$$

There are several types of interpolation linear,nearest neighbor, cubic spline, piece-wise cubic hermite and cubic interpolation and depending on the channel statistics the suitable technique should be chosen.

Last, time averaging is done to smooth the channel transition from one symbol to another and to decrease the effect of erroneous channel estimates.

$$\mathbf{H}_t = \left(1 - \frac{1}{\alpha}\right)\mathbf{H}_{t-1} + \frac{1}{\alpha}\mathbf{H}_{up} \tag{4.8}$$

where α is the forgetting factor.

$$\hat{S}_{T,t}(k) = \frac{S_{R,t}(k)}{H_t(k)}. \tag{4.9}$$

4.4.2 Co-Pilot Interpolation Estimator

Relying only on interpolation between pilots is not efficient as the the pilots provided for the IEEE 802.11p standard are not sufficient to sample the channel in frequency domain. Data decision feedback is used to estimate the channel on non pilot subcarriers assuming that the data is demodulated correctly. In order to combat the unreliability of this assumption, three techniques are done to make the channel estimates more reliable and accurate. First,Redundancy is achieved by using several data subcarriers to calculate channel estimate at each subcarrier. Second,averaging multiple channel measurements to reduce the effect of noise and erroneous channel estimates. Third, Depending on the channel variation whether it is slow or fast, the channel update rate is adjusted accordingly in order to cancel out the effect of erroneous channel estimates by putting more weight on previous estimates and prevent sudden changes in case of slow channel characteristics. On the other hand, if the update rate is too slow the estimator won't be able to track fast channel variations. That's why the update rate must be chosen very carefully depending on the channel coherence time.

Co-Pilot interpolation estimator is done by forming evenly spaced copilots from the data information in subcarriers. Following are the steps needed to perform the channel estimation and tracking. First, symbol demodulation is done after equalization using the previous channel estimate

$$\hat{S}_{T,t}(k) = \frac{S_{R,t}(k)}{H_{t-1}(k)}. \tag{4.10}$$

Second, an initial channel estimate is calculated using the received symbol and the demodulated data obtained

$$H(k) = \frac{S_{R,t}(k)}{X(k)}. \tag{4.11}$$

Third, copilots are formed by linear combination of channel estimates of the data sub-carriers in its vicinity as shown below

$$H_{cp}(\lambda) = \sum_{k=-\beta}^{\beta} w_k H(\lambda + k) \tag{4.12}$$

where w_k represents the weights given to each subcarrier.

Fourth, The necessary copilots are extracted to form an evenly spaced pilots and copilots then they pass through an interpolation circuit. By comparison it was found that $L = 3$ copilot spacing is better than $L = 7$ and the weights used are $w_1 = W_{-}1 = 0.25$ and $w_0 = 0.5$

$$H_{cp}(\lambda) = \sum_{k=-1}^{1} w_k H(\lambda + k) = 0.25 H(\lambda - 1) + 0.5 H(\lambda) + 0.25 H(\lambda + 1). \tag{4.13}$$

Also note that pilot subcarriers are intuitively could take higher weights than regular copilots.

Last, the output of the interpolation circuit is used to update the moving average in time in order to get the channel estimates needed for equalization

$$\mathbf{H}_t = \left(1 - \frac{1}{\alpha}\right)\mathbf{H}_{t-1} + \frac{1}{\alpha}\mathbf{H}_{up}. \tag{4.14}$$

4.4.3   Spectral Temporal Averaging (STA)

To be able to track the time varying channels characteristics, the STA technique was presented in [5]. STA is based on the correlation between each subcarrier and its neighboring subcarriers in the frequency domain as well as the time correlation between successive OFDM symbols. STA is done as follows. First, the LS estimate $\hat{H}_{LS}$ is used as an initial estimate then data decision feedback is done by demodulating the first data symbol compensated by the LS initial estimate as follows

$$\hat{S}_t(k) = \frac{Y_t(k)}{\hat{H}_{t-1}(k)} \tag{4.15}$$

where $\hat{S}_t(k)$ is the equalized symbol at subcarrier k and time t, $Y_t(k)$ is the received symbol at subcarrier k and time t and $\hat{H}_{t-1}(k)$ is the channel estimate of the previous symbol. A more accurate channel estimate is calculated using the demodulated data as

shown below

$$\hat{H}_t(k) = \frac{Y_t(k)}{\hat{X}_t(k)} \tag{4.16}$$

where $\hat{X}_t(k)$ is the demodulated symbol from $\hat{S}_t(k)$. The frequency domain correlation between neighboring subcarriers is exploited by the below formula

$$H_{up,\,t}(k) = \sum_{i=-\beta}^{\beta} W_i \hat{H}_t(k+i) \tag{4.17}$$

where $H_{up,\,t}$ is the updated channel estimate based on the correlation between neighboring subcarriers, β is the window size where the weighted average takes place and W_i is the weight of each subcarrier in the window. Then the time domain averaging is done as follows

$$\mathbf{H}_{STA,\,t} = \left(1 - \frac{1}{\alpha}\right) \mathbf{H}_{STA,\,t-1} + \frac{1}{\alpha} \mathbf{H}_{up,\,t} \tag{4.18}$$

where α is called the forgetting factor and it is optimized based on the maximum Doppler of the channel. These parameters are adjusted according to the varying channel characteristics however this is not an easy job in practice so these parameters are optimized offline then fixed for simplicity with sacrifice in terms of performance degradation.

4.4.4 Performance Comparison

Spectral Temporal averaging and Co-pilot interpolation algorithm achieve good performance at stationary environments even with relatively large packets, However fails to track channel variation at high doppler environments.

Pilot interpolation is the most suitable algorithm in the comb type for dynamic environments but still a lot can be achieved.

FIGURE 4.6: BPSK Bit Error Rate, maximum doppler=200Hz and 50 OFDM symbol per packet.
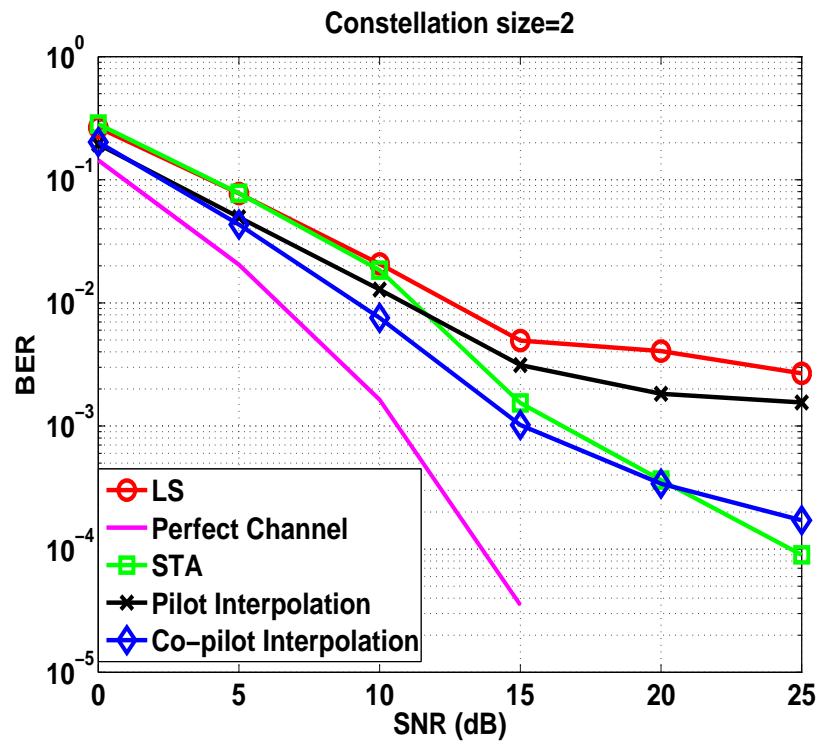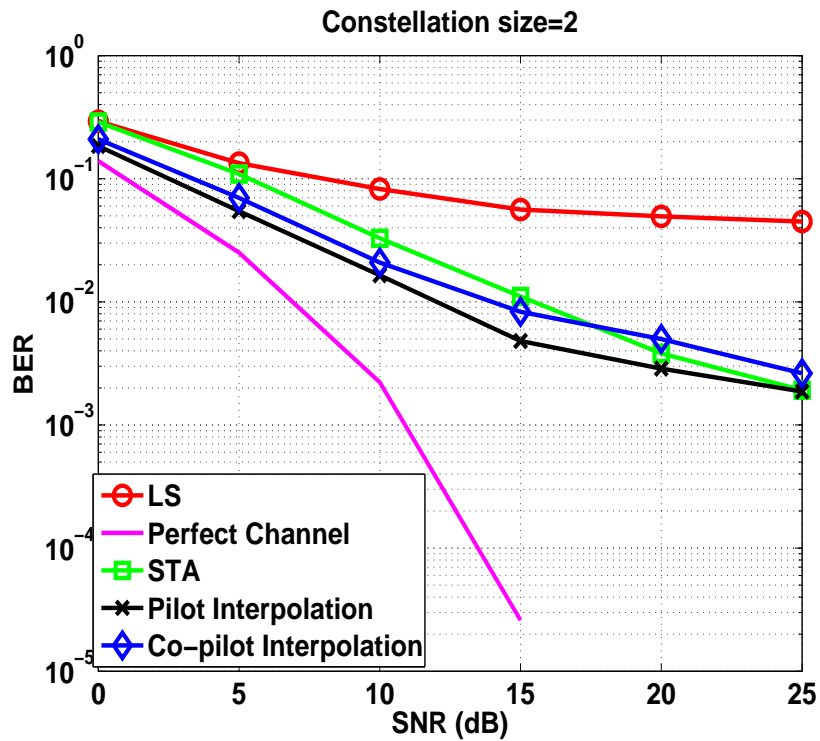
FIGURE 4.7: BPSK Bit Error Rate, maximum doppler=500Hz and 50 OFDM symbol per packet.
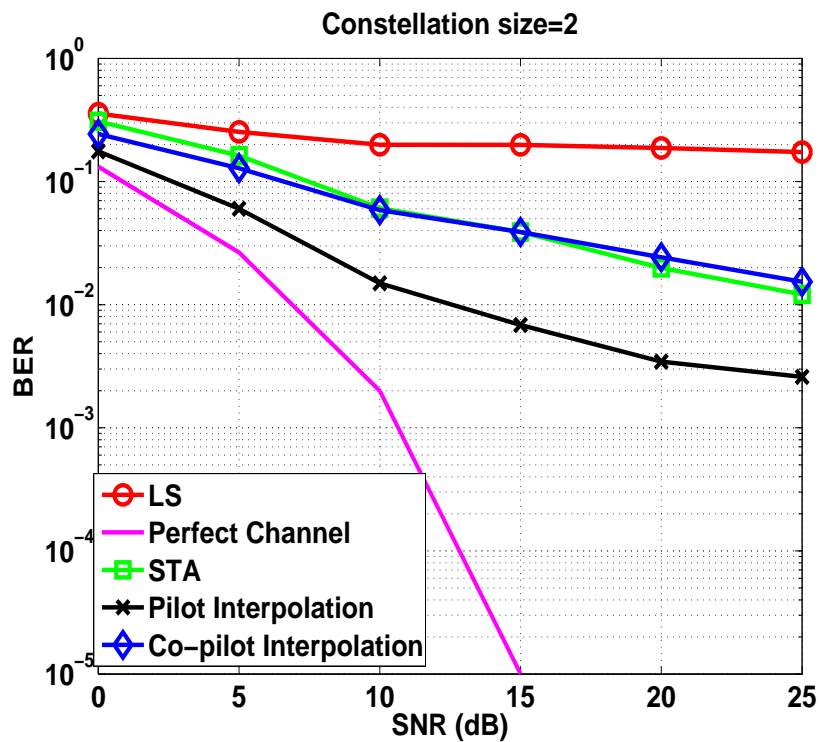

FIGURE 4.8: BPSK Bit Error Rate, maximum doppler=1000Hz and 50 OFDM symbol per packet.
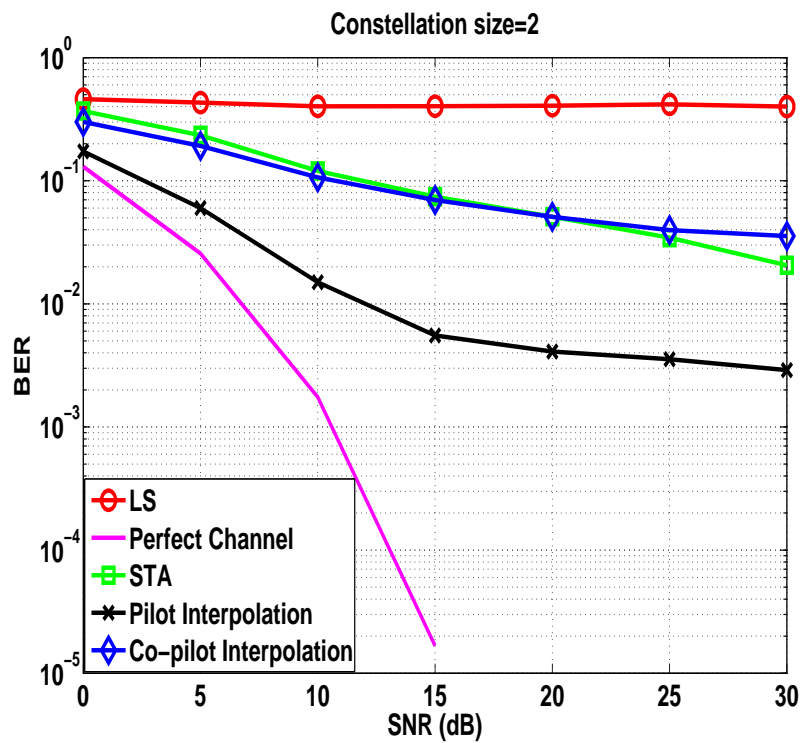
FIGURE 4.9: BPSK Bit Error Rate, maximum doppler=1000Hz and 100 OFDM symbol per packet.
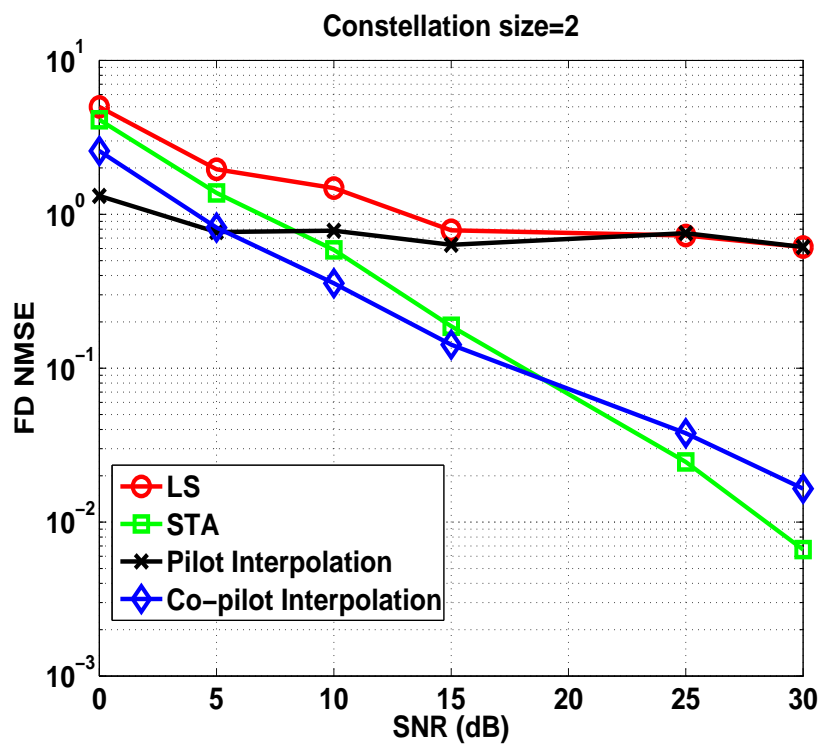

FIGURE 4.10: BPSK Mean Square Error, maximum doppler=500Hz and 100 OFDM symbol per packet.

4.5   Blind Channel Estimation

In literature, blind channel estimation techniques are used only if the channel is static over a long enough period to achieve a reliable statistical behavior of the received signals. That is why totally blind estimation techniques are unusable in fast fading channels.

The insufficient pilots in the IEEE 802.11p OFDM symbols motivated the use of semi-blind techniques. Applying the suitable techniques along with the pilot information and channel characteristics is promising.

4.5.1   Finite Alphabet

Using the work of [49],

$$S(i) = [S(iM), S(iM + 1), ..., S(iM + M - 1)]^T \tag{4.19}$$

where $S(i)$ is the information stream, i is the OFDM symbol index and M is the number of subcarriers in the OFDM symbol.

The output in the frequency domain is as equation (2.1), repeated for convenience

$$Y(i, m) = H(\rho_m)S(i, m) + Z(i, m) \tag{4.20}$$

where m is the subcarrier index, Z is the Gaussian noise. Under the following assumptions: 1.Symbols are drawn from a finite alphabet set of size Q; $S(i, m) \in \{\mathcal{S}_q\}_{q=1}^Q$ 2.Symbols are equiprobable; $Pr(s(i, m) = \epsilon_q) = 1/Q$, for $q = 1, 2, ..., Q$ 3.Noise is zero mean complex circular Gaussian and independent of s(i,m).

Clearly,

$$\Pi_{q=1}^Q [S(i, m) - \mathcal{S}_q] = 0 \tag{4.21}$$

where $S(i, m)$ must be $\in$ of the $\mathcal{S}_q$'s.

Working with the product of terms, we obtain

$$S^Q(i, m) + \alpha_1 S^{Q-1}(i, m) + ... + \alpha_Q = 0 \tag{4.22}$$

where α_i's are the polynomial coefficients. α_i's are constellation dependent.
For PSK $J = Q$ & $\alpha_J = 1$ and all of the other α_i's= 0, where J is the smallest index of non zero coefficient α_i.
$J = 2$ for BPSK and $J = 4$ for QPSK,16 QAM and any higher order QAM.

Under the first two assumptions,

$$E[S^J(i,m)] = \frac{-J}{Q}\alpha_J \neq 0. \tag{4.23}$$

For PSK $E[S^J(i,m)] = \frac{-J}{Q}\alpha_J = -1$ deterministically for any $S(i,m)$.

Since we deal with complex noise

$$E[Z^n(i,m)] = 0, \quad \forall \ n > 0. \tag{4.24}$$

Taking the expectation of (4.20)

$$E[Y^J(i,m)] = H^J\rho_m E[S^J(i,m)]. \tag{4.25}$$

Substituting $E[S^J(i,m)]$ with $\frac{-J}{Q}\alpha_J$ according to (4.23)

$$H^J(\rho_m) = \frac{-Q}{J\alpha_J}E[Y^J(i,m)]. \tag{4.26}$$

We need to get $h(l)$ from $H^J\rho_m$.

Let $\beta_J^T = [\beta_0, ..., \beta_{JL}]$

$$H^J(\rho_m) = H^J(Z) \mid_{Z=\rho_m} = (\beta_0, ..., \beta_{JL}Z^{-JL}) \mid_{Z=\rho_m}. \tag{4.27}$$

To get β_J^T, we need $JL + 1$ equations for $JL + 1$ distinct values of ρ_m, so selecting $M \geq JL + 1$ allows to find β_J^T uniquely. Also, $H^J(Z) = \sum_{i=0}^J L\beta_i Z_i$ we can determine $H^J(Z)$ on entire complex plane as $H^J(Z)$ contains all roots of $H(Z)$ with multiplicity J. Eventually, we can extract the L roots to form $H(Z)$.

$$\begin{aligned}
\hat{H}^J(\rho_m) &= \frac{-Q}{J\alpha_J}\left(\frac{1}{I}\sum_{i=0}^{I-1}Y^J(i,m)\right), m \in [0.M-1] \\
&= V_J\beta_J
\end{aligned} \tag{4.28}$$

where I is the total number of blocks, $V_J = \sqrt{M}F_M(:, 1 : JL+1)$, F_M is the DFT matrix of size M and $\beta_J = \frac{1}{M}V_J^H$.

Relying on equations 4.20 and 4.28 sufficient information is provided to recover the channel vector $h = [h(0), ..., h(L)]^T$.

4.5.1.1 FA

Starting from the frequency domain, channel estimation could be done as follows

$$\hat{H}(\rho_m) = \lambda_m [\hat{H}^J(\rho_m)]^{\frac{1}{J}} \tag{4.29}$$

where $\lambda_m \in \exp^{j(\frac{s\pi}{J})n}{}_{n=0}^{J-1}$ is the corresponding scalar ambiguity in taking the Jth root. To resolve these ambiguities, exhaustive search is done over all J^M possible vectors

$$\hat{\tilde{h}}_1 = [\lambda_0 [\hat{H}^J(\rho_0)]^{\frac{1}{J}}, ..., \lambda_{M-1}[\hat{H}^J(\rho_{M-1})]^{\frac{1}{J}}]^T. \tag{4.30}$$

The corresponding time domain vector is computed as follows

$$\hat{h}_1 = V_1^\dagger \hat{\tilde{h}}_1 = \frac{1}{M} V_1^H \hat{\tilde{h}}_1 \tag{4.31}$$

where V_1 is a scaled version of the first $L+1$ columns of FFT matrix

$$V_1 = \sqrt{M} F_M(:, 1:L+1). \tag{4.32}$$

Channel estimates are then found by minimizing the Euclidean distance

$$\hat{h} = \arg\min_{\hat{h}_1} ||\hat{\beta}_J - \hat{h}_1 *_J \hat{h}_1||. \tag{4.33}$$

Since the channel order $L < M$.

To obtain the time domain channel estimate $\hat{\tilde{h}}_1$, select $\bar{N}$ elements from $\hat{\tilde{h}}_1$ and form a new $\bar{N}$x1 vector $\tilde{\tilde{h}}$.

So now we only need to search over $J^{\bar{N}}$ instead of all J^M possible vectors, where $\bar{N} \geq L+1$ chosen to form equispaced subcarriers.

$$\hat{h}_1 = \bar{V}^T \tilde{\tilde{h}} \tag{4.34}$$

where $\bar{V}$ is constructed from V_1 by keeping only the corresponding $\bar{N}$ rows.

4.5.1.2 Sliding Window

In order to decrease the effect of the additive noise, block averaging is done. We form a sliding window (rectangular shape of size$W$) channel estimates by averaging only the W most recently received blocks $Y(i)_{i=I-W+1}^{I}$.

A trade-off exist between reduced variance estimation and enhanced tracking capability in the window size choice.

$$\hat{H}^J(k) = \gamma \frac{1}{I} \sum_{i=0}^{I-1} Y^J(i;k) \tag{4.35}$$

where γ is a constant used to remove the data effect from the channel estimates.

4.5.1.3 Over Estimated Channel Order L=10,N=12

According to [34] the time domain channel model for V2V communication has 8 taps. We can try over estimating the channel order and study it's effect. Also the effect of increasing $\bar{N}$ depending on the following condition $\bar{N} \geq L + 1$ must be studied as in order to decrease the algorithm complexity $\bar{N} = L + 1$ is used. The simulation results shows the effect of increasing both of the above parameters.

4.5.1.4 Time Truncation

In order to exploit the time domain channel characteristics of the V2V environment, time truncation is used to boost the channel estimation and tracking capabilities as well as resolving the phase ambiguities of the channel frequency response. Truncating the channel estimates in the time domain higher than the 8th tap defined by the V2V channel model and then back and forth between the frequency and time domains until convergence. The effect of channel noise (and thus channel estimation error) in the frequency domain are reflected as higher number of taps in the time domain that is why truncating the channel impulse response enhance channel estimation performance.

It was found by simulation that this loop converges after a few number of iterations so it could be fixed at only two iterations. On the other hand, this technique increases the channel tracking capabilities even with a coarse initial estimate in a highly dynamic environment.

Each iteration entails one M point $IFFT$ and one M point FFT. As $M = 64$, so this technique has a low computational complexity for the IEEE 802.11p standard.

The phase ambiguities are resolved by searching over J candidate phase values as follows

$$H_{freq}(k) = \arg \min_{\lambda_m [\hat{H}^J(k)]^{1/J}} ||H_{freq}(k) - \lambda_m [\hat{H}^J(k)]^{1/J}|| \tag{4.36}$$

where $H_{freq}(k)$ is the initial channel estimates in the frequency domain and $\hat{H}^J$ is the received signal raised to the Jth power to eliminate the data effect.

$$h_{time} = IFFT(H_{freq}), \tag{4.37}$$

$$H_{freq} = FFT(h_{time}(1:8)), \tag{4.38}$$

then the pilots majority rule is used again as the channel estimates may converge at wrong polarity.

4.5.1.5 Finite Alphabet with Time Truncation (FA-TT) Algorithm

A new semi-blind channel estimation algorithm is presented based on the previous blind channel estimation techniques. Due to the fast varying channel characteristics, trying to track the channel variations using the two long training sequences and the LS estimates would not be able to do the job. That is why blind channel estimation techniques would be a key to estimate the channel more accurately. Totally blind channel estimation techniques in [49] will not solve the phase ambiguities in the channel estimates and therefore cannot be used for data equalization. Moreover, the semi-blind application of the algorithm in [49] is able only to track the slow channel variations and when the channel varies with time a significant SNR loss occurred and to decrease this loss frequent training is needed along with long bursts of data which is not applicable if we are trying to be complaint to the 802.11p standard.

In the proposed technique we exploit the pilots information in each OFDM symbol to determine the channel polarity and also the number of channel taps in time domain is exploited to boost the performance by time domain channel truncation technique.

The initial channel estimates are obtained based on the finite alphabet property of the transmitted data symbols as follows [49]

$$\hat{H}^J(k) = \gamma \frac{1}{I} \sum_{i=0}^{I-1} Y^J(i;k) \tag{4.39}$$

where J equals 2 in case of BPSK and 4 in all higher order constellations, γ is a constant used to remove the data effect from the channel estimates so γ equals to 1 for BPSK,

-1 for QPSK but for higher order constellations it must be calculated for each symbol as the reciprocal of the symbol raised to the Jth power, I is the block size and Y is the received symbol at the kth subcarrier at time i. In the new algorithm a block size of 3 OFDM symbols is used to decrease the noise effect and also be able to track the fast channel variations. Then

$$\mathbf{\Phi} = \text{IFFT}(\hat{H}^J). \tag{4.40}$$

If we ignore the noise $\hat{H}^J$ is the perfect channel raised to the Jth power and the $\mathbf{\Phi}$ is the J-fold convolution of the perfect channel in the time domain so $\mathbf{\Phi}$ could be used as reference in case of noisy channel estimates.

An exhaustive search over all the combinations of any eight equally spaced subcarriers is done in order to get the 8-tap channel in the time domain then a J-fold convolution is calculated and the distance between $\mathbf{\Phi}$ and each of the Q^8 combinations, where Q is the constellation size, is calculated and the minimum distance will be the initial estimate for our algorithm as shown below

$$\mathbf{\hat{H}_1} = \lambda_m [\hat{H}^J(k)]^{1/J} \tag{4.41}$$

where λ_m is the corresponding scalar ambiguity when taking the Jth root (which can be resolved later using the 4 pilot symbols in each OFDM symbol).

$$\mathbf{\hat{h}_{init}} = \arg\min_{\hat{h}_1} ||\Phi - \hat{h}_1 *_J \hat{h}_1|| \tag{4.42}$$

where $\hat{h}_1 = \text{IFFT}(\hat{H}_1)$ and $*_J$ denotes the J-fold convolution; then the 8-tap channel estimates $\hat{h}_1$ are FFT processed to be converted to 64-subcarrier frequency response

$$\mathbf{H_1} = \text{FFT}(\hat{h}_1). \tag{4.43}$$

Majority rule is used to solve the polarity ambiguity of the channel impulse response (as the distance of the channel and its negative value is the same; can not be resolved using equation (4.42) only) by comparing the initial channel estimates ($\mathbf{H_1}$) of the 4 pilot symbols with their LS channel estimates. And if the majority of the pilots LS channel estimates have the same polarity as the pilots' initial channel estimates so no change in the initial channel estimates' polarity. Otherwise, the polarity of all initial channel estimates must be inverted.

The phase ambiguities of the channel frequency response are resolved by modifying the channel of each subcarrier according to equation (12) and truncating the IFFT of the channel in the time domain by removing the taps after the eighth tap then iterate until

there is no change in the subcarriers coefficients.

$$\hat{\mathbf{H}}_{\mathbf{FA-TT}} = \arg \min_{\lambda_m [\hat{H}^J(k)]^{1/J}} ||\hat{H} - \lambda_m [\hat{H}^J(k)]^{1/J}|| \tag{4.44}$$

where $\hat{H} = \text{FFT}(\hat{h}_{init})$. Then the pilots majority rule is used again as the channel estimates may converge at wrong polarity.

It was found by simulation that this loop converges most of the time after only two iterations so we can fix it at 2. The problem with this algorithm is that the computational complexity increases vastly as the modulation order increases which makes it practical only for the BPSK case.

4.5.1.6 Performance Comparison

Simulation results show that over estimating the number of channel taps in the time domain in order to get a better initial estimate decrease the performance of the algorithm as well as

The use of the sliding window technique increase the performance of the FA-TT algorithm with 3-5 dBs. Both algorithm achieve a very good performance in terms of overall bit error rate for low and high mobility environments with all packet sizes.
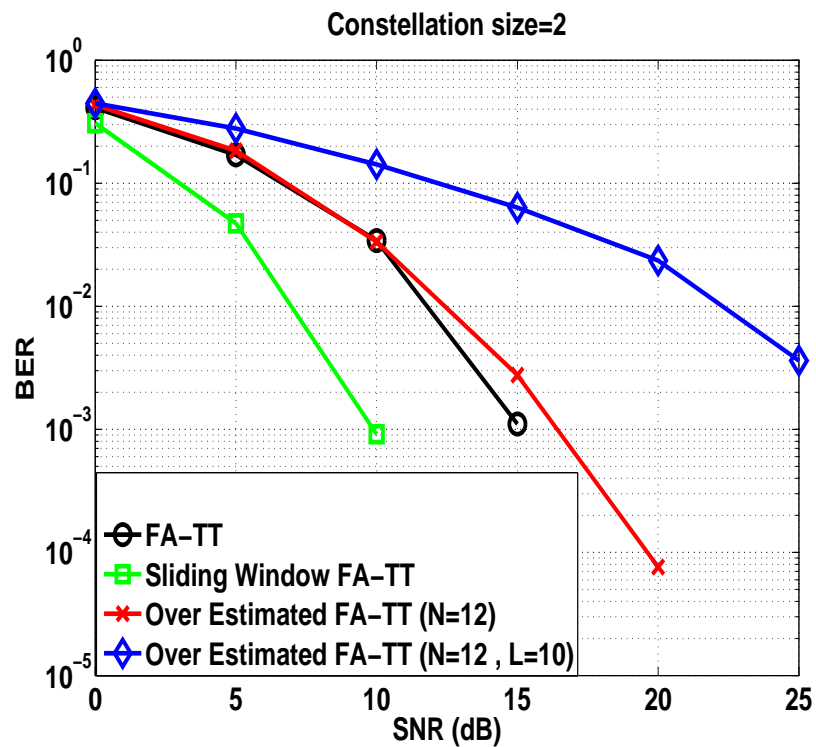

FIGURE 4.11: BPSK Bit Error Rate, maximum doppler=200Hz and 50 OFDM symbol per packet.
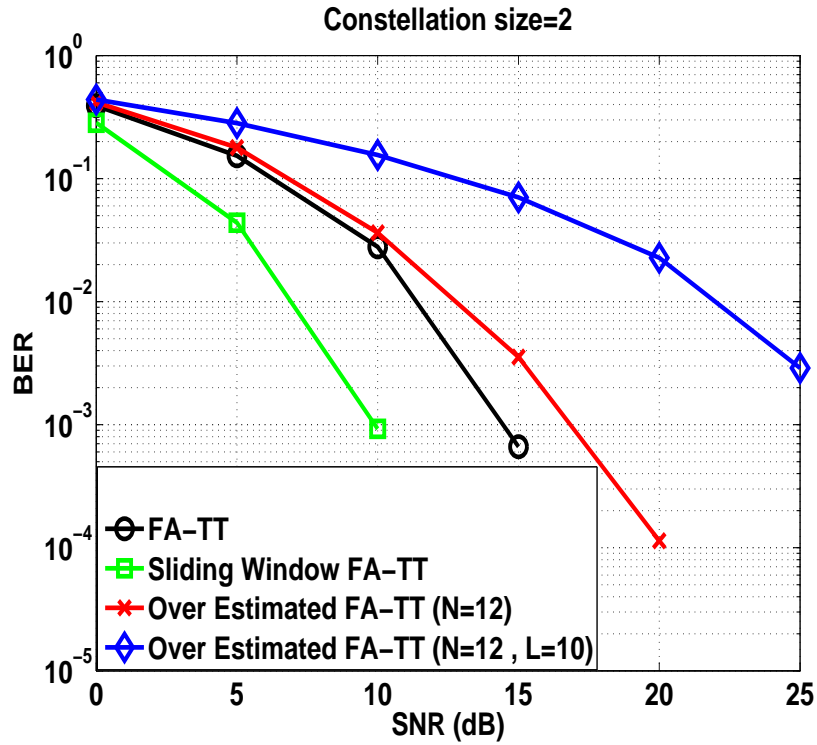
FIGURE 4.12: BPSK Bit Error Rate, maximum doppler=500Hz and 50 OFDM symbol per packet.
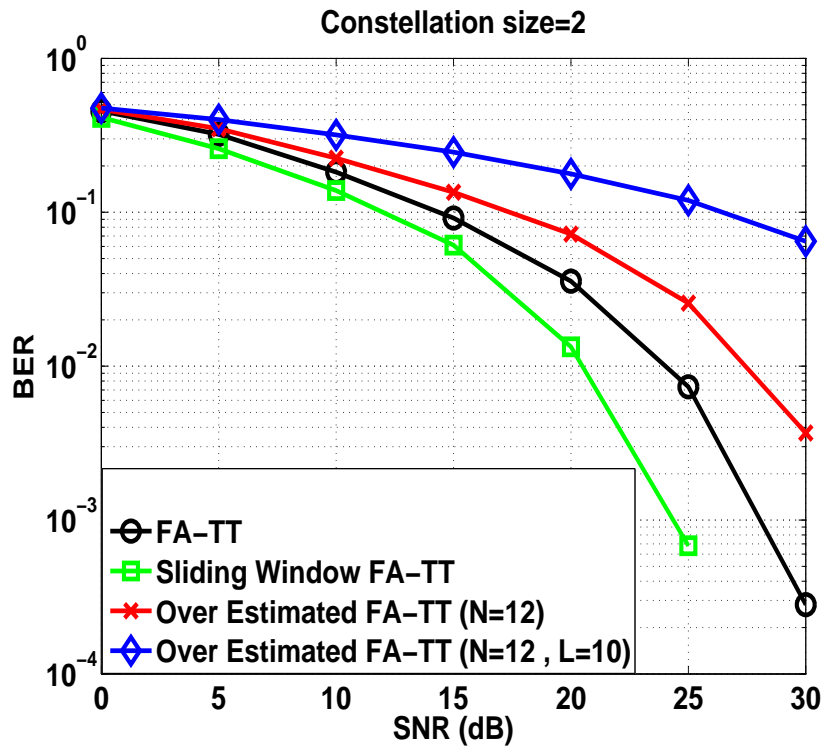

FIGURE 4.13: BPSK Bit Error Rate, maximum doppler=1000Hz and 100 OFDM symbol per packet.
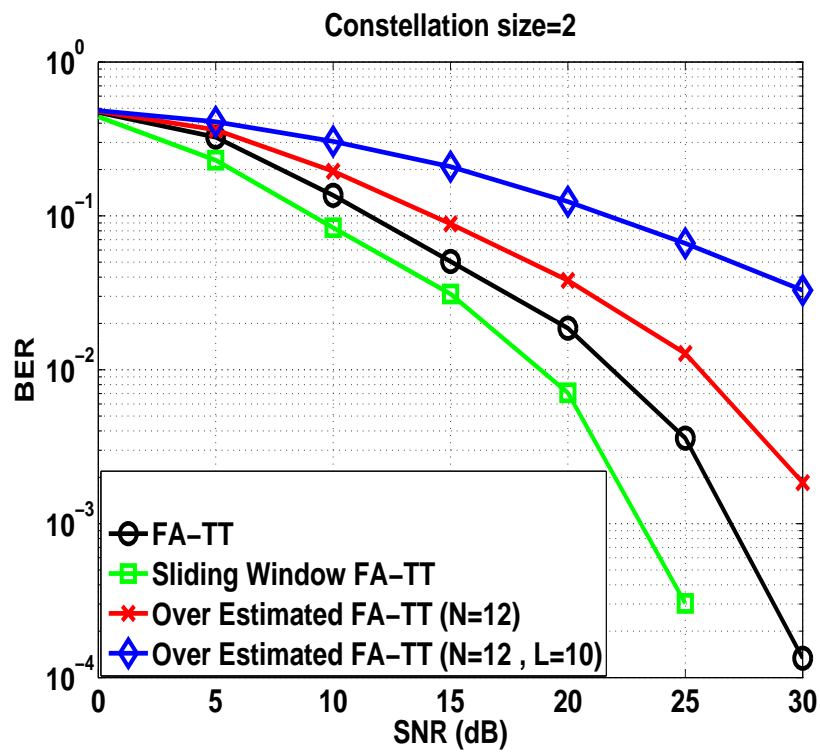
FIGURE 4.14: BPSK Bit Error Rate, maximum doppler=1000Hz and 200 OFDM symbol per packet.

4.5.2   Pilot Aided

Pilot aided schemes in general are discussed in [50, 51, 52, 53].

4.5.2.1   fixed pilots' response Time Truncation

In order to benefit from the channel information at the pilots' subcarriers and also to make sure that channel response truncation in the time domain won't affect the channel estimates at the pilots' positions, this algorithm was developed keeping that in mind.

The initial channel estimates are calculated based on the finite alphabet property as described before. The only difference in this algorithm is that in the time truncation process, we make sure that the channel estimates at pilots' positions are kept unchanged.

4.5.2.2   Low Complexity FA

The complexity of the FA algorithm is directly proportional to $J^{\bar{N}} \geq J^{L+1}$ which makes the algorithm affordable only for low order channels as well as limited constellation sizes.

To decrease the complexity, pilot tones are used. As a result of this we only need to search over $J^{\bar{N}-N_P}$ where N_P is the number of pilots in the OFDM symbols.

4.5.2.3   Pilot Interpolation-TT

For the sake of a low complexity algorithm, Pilot Interpolation-TT algorithm was developed. The initial channel estimate is calculated by interpolating the channel estimates at the pilots' positions then this initial estimate is further enhanced by time truncation iterations.

4.5.2.4   Previous-TT

The training sequences are used in this algorithm to provide the time truncation process with an initial channel estimate and after the first OFDM symbol, the channel estimates of the previous OFDM symbol are used to initialize the time truncation iterations for the coming OFDM symbol.

4.5.2.5 Performance Comparison

Simulations results shows that using the pilots to decrease the algorithm complexity by searching over only 2^4 combinations vastly degrades the performance, also fixing the channel response at pilots' positions in time truncation iterations has bad impact on performance.

Pilot interpolation and Previous Symbol CR-TT algorithms have good performance at stationary environments with relatively large packets but when the doppler values go beyond 500 Hz, the algorithms fail to track the channel variations.
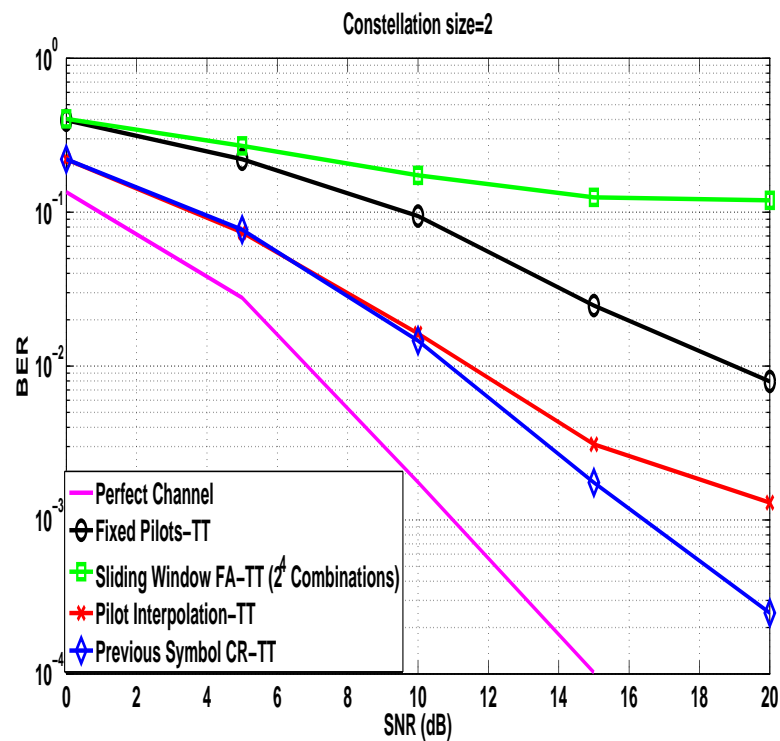

FIGURE 4.15: BPSK Bit Error Rate, maximum doppler=200Hz and 50 OFDM symbol per packet.
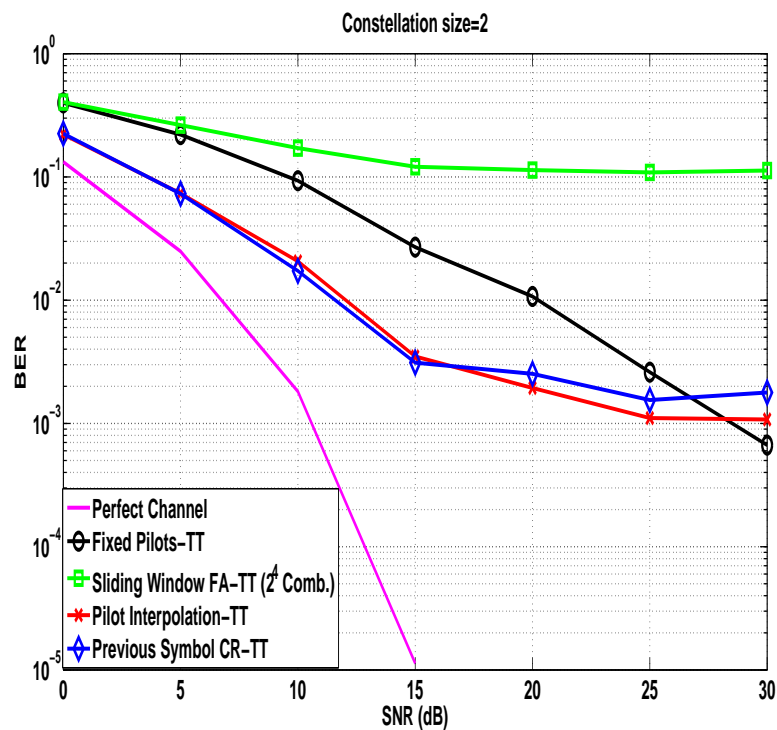
FIGURE 4.16: BPSK Bit Error Rate, maximum doppler=500Hz and 50 OFDM symbol per packet.
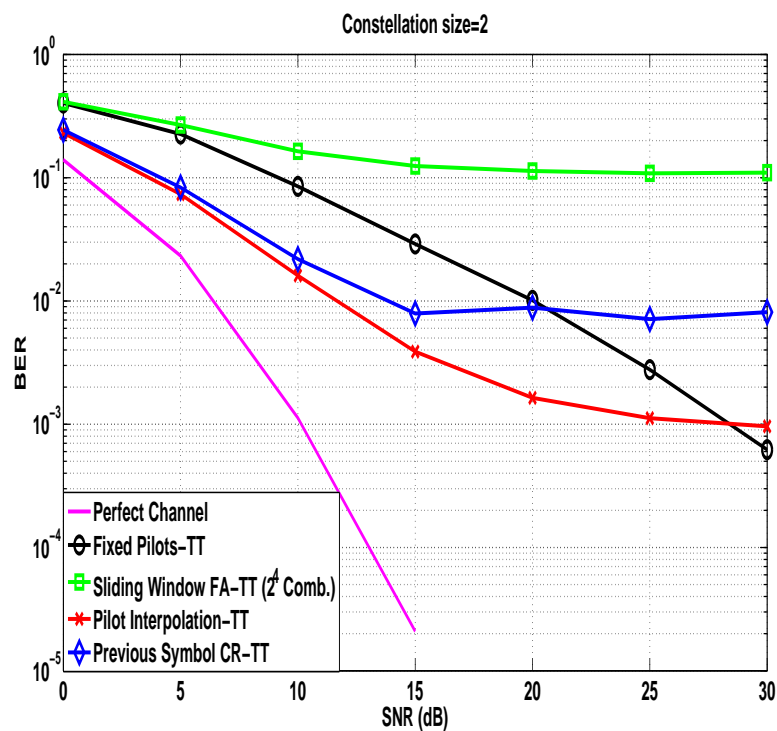

FIGURE 4.17: BPSK Bit Error Rate, maximum doppler=1000Hz and 100 OFDM symbol per packet.
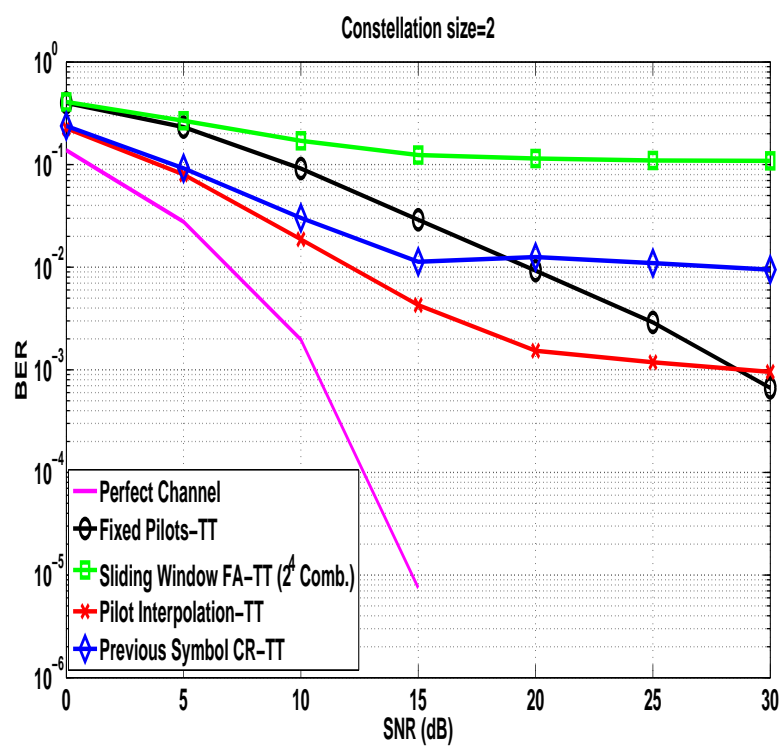
FIGURE 4.18: BPSK Bit Error Rate, maximum doppler=1000Hz and 200 OFDM symbol per packet.

4.6 Semi Blind Channel Estimation

4.6.1 Minimum Distance Estimator

By digging deeper into the IEEE 802.11p standard, and trying to find a simple algorithm that can solve the performance issue at highly mobile environment, the proposed algorithm was developed intuitively keeping complexity and performance in mind. This estimator has a low computational complexity and the ability to track fast channel variations by exploiting the channel estimates at the four pilots in every OFDM symbol as well as the high correlation characteristic of the channel response between adjacent subcarriers .

First the 48 data subcarriers are divided into four groups. Each group has the pilot subcarier in the middle.

Starting from the pilot position, the channel estimates of the neighboring subcarrier are determined based on the minimum Euclidean distance between the pilot channel estimate and the possible channel responses of its neighboring subcarrier according to the below equations (depending on the relative location to the pilot, if the subcarrier is on the rightside of the pilot use equation (4.45) otherwise use equation (4.46)).

Using the estimated channel response of the neighboring subcarrier to estimate the subcarrier next to it and so on until all the neighboring subcarriers in the pilot's group are scanned and then we move on to the second pilot position.

$$H_{freq}(k+1) = \arg \min_{\lambda_m[\hat{H}(k+1)]} ||H_{freq}(k) - \lambda_m[\hat{H}(k+1)]||, \qquad (4.45)$$

$$H_{freq}(k-1) = \arg \min_{\lambda_m[\hat{H}(k-1)]} ||H_{freq}(k) - \lambda_m[\hat{H}(k-1)]|| \qquad (4.46)$$

where λ_m is the corresponding ambiguity in the channel response based on the constellation used in data transmission ($\lambda_m \in \{\pm 1\}$ for BPSK and $\lambda_m \in \{\pm 1, \pm j\}$ for QPSK).

4.6.2 Minimum Distance Estimator with time truncation

To enhance the tracking capabilities of the Minimum Distance Estimator, time truncation is done to exploit the information about the channel taps in the time domain. The

Minimum distance estimator provides the time truncation algorithm with the initial estimate, time truncation iterations enable the estimator to track fast channel variations more closely and yet the complexity of the overall estimator is still low.

4.6.3 Sliding Time Truncation

This Algorithm provides an initial estimate with a reduced noise variance to the time truncation estimator.

Noise variance reduction is done by a simple rectangular sliding window as described before in section 4.4.1.2.

4.6.4 Performance Comparison

Minimum distance and Minimum distance with time truncation algorithms achieve a very good performance in stationary environments and also are able to track fast channel variations in vehicular environments even with very large packet sizes.

The low computational complexity of both algorithms makes them suitable for V2V applications which require fast yet efficient algorithms to meet the critical timing limits of safety real time applications.
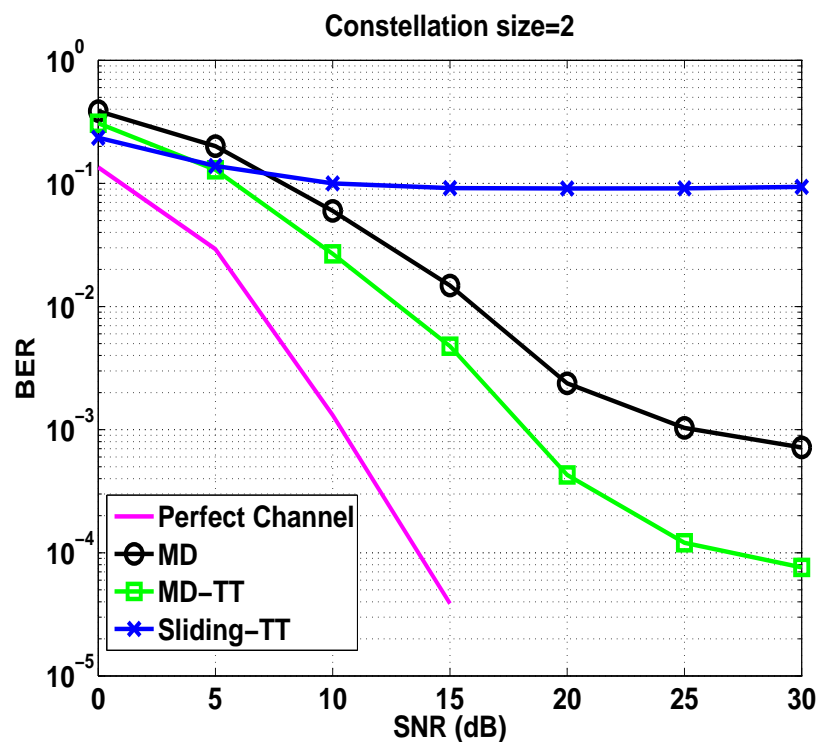

FIGURE 4.19: BPSK Bit Error Rate, maximum doppler=200Hz and 50 OFDM symbol per packet.
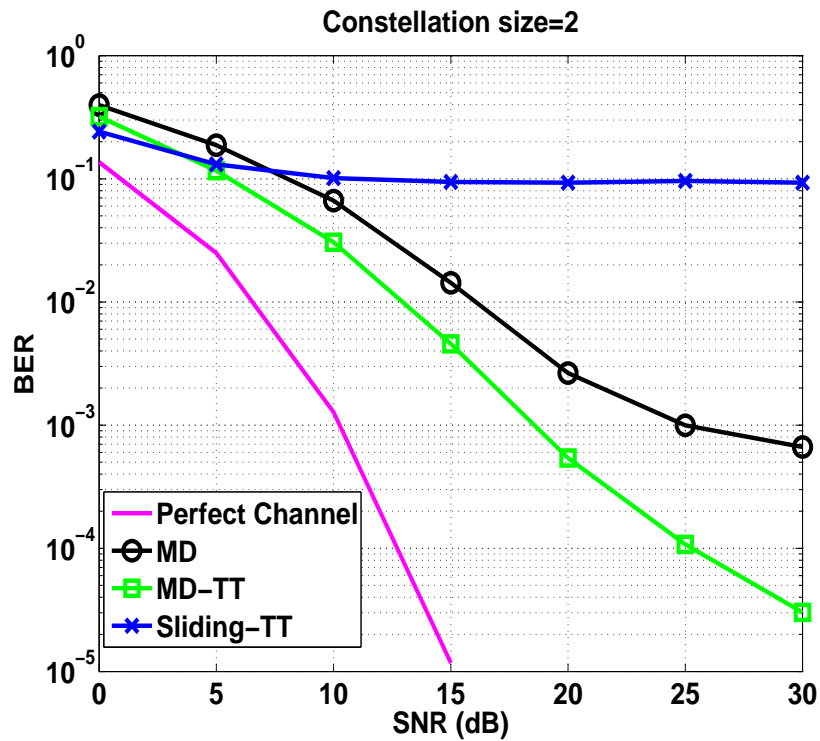
FIGURE 4.20: BPSK Bit Error Rate, maximum doppler=500Hz and 50 OFDM symbol per packet.
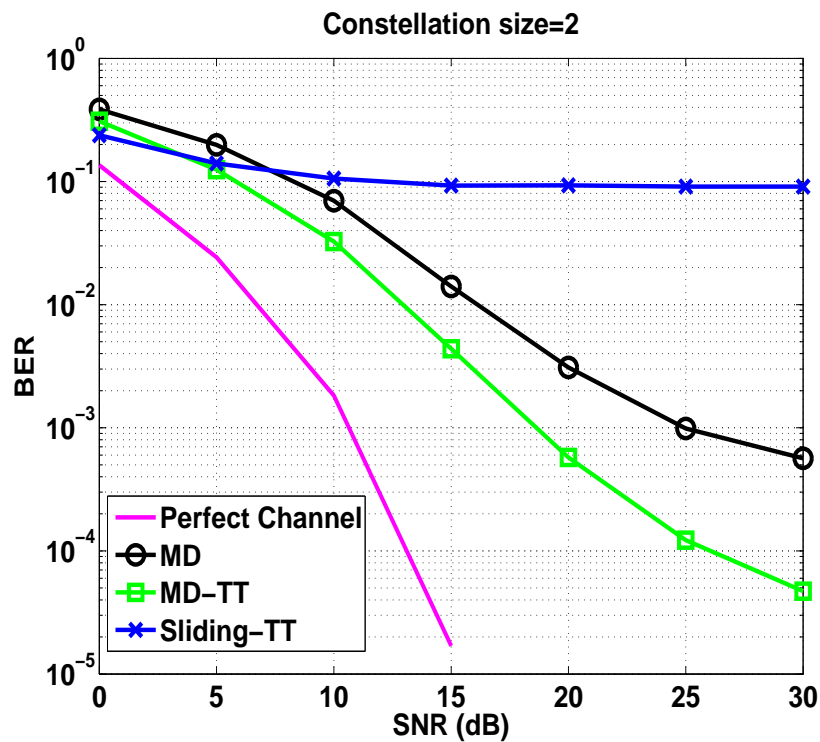

FIGURE 4.21: BPSK Bit Error Rate, maximum doppler=1000Hz and 100 OFDM symbol per packet.
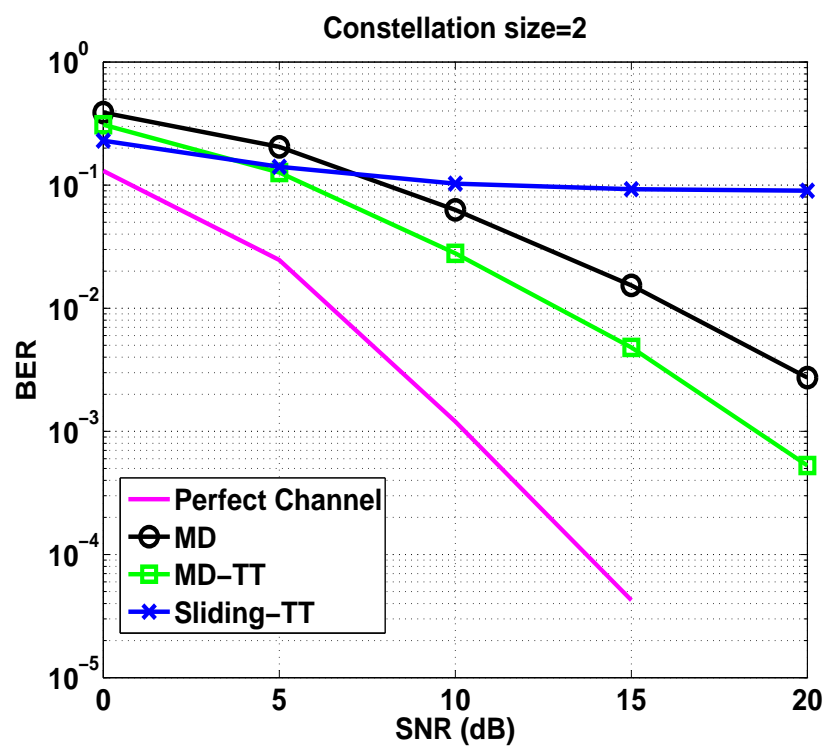
FIGURE 4.22: BPSK Bit Error Rate, maximum doppler=1000Hz and 200 OFDM symbol per packet.

4.7 Decision Directed Channel Estimation

Decision-directed channel estimation was extensively covered in literature [54, 55, 56, 57, 58, 59, 60], and has been demonstrated to have an advantage over pilot aided schemes in terms of performance and bandwidth efficiency. On the other hand, in order to design decision-directed channel estimation, a decision feedback of desired data is needed and error propagation is one of the major problems that should be avoided when using decision-directed channel estimation specifically at low SNR. A wrong decision due to noise or channel fading can result in an unreliable channel estimate. As a result, signal compensation produces more errors in data that produce another wrong decision. This results in the loss of the entire packet.

4.7.1 Constructed Data Pilots (CDP) Estimator

Exploiting the correlation between adjacent symbols the CDP estimator achieves a higher performance than STA at high SNR. The CDP estimator consists of four steps, the last two steps are the different ones from the STA. First, the CDP estimator uses the channel response of the previous symbol to update the channel estimate as follows

$$\hat{S}_i(k) = \frac{Y_i(k)}{H_{CDP,i-1}(k)}.$$ (4.47)

Second, data pilots $\hat{X_i}(k)$ are constructed by demodulation of the equalized symbol. then an initial is calculated using LS estimation

$$\hat{H}_i(k) = \frac{\hat{S}(k)}{\hat{X_i}(k)}.$$ (4.48)

Third, $\hat{H}_i(k)$ and $H_{CDP,i-1}(k)$ are used separately to equalize the previous symbol as shown

$$\hat{S}'_{i-1}(k) = \frac{\hat{S}_{i-1}(k)}{\hat{H}_i(k)},$$ (4.49)

$$\hat{S}''_{i-1}(k) = \frac{\hat{S}_{i-1}(k)}{\hat{H}_{CDP,i-1}(k)}.$$ (4.50)

Fourth, A Comparison between the demodulated data from equation 4.49 and equation 4.50 ($\hat{X}_{i-1}(k)'$ & $\hat{X}_{i-1}(k)''$) is done. Depending on the high correlation between adjacent

data symbols, if $\hat{X}_{i-1}(k)' \neq \hat{X}_{i-1}(k)''$ therefore $\hat{X}_i(k)$ is not correct and $H_{CDP,i}(k) = H_{CDP,i-1}(k)$. Otherwise, $H_{CDP,i}(k) = H_i(k)$.

The only exception to the previous equations is that for the first data symbol received $\hat{S}_{i-1}(k)$ equals the second long training symbol and $X_{\hat{i-1}}(k)''$) is the known transmitted pilots in the frequency domain.

4.7.2 Iterative Decision Directed Estimator

This Algorithm depends on decision directed channel estimation. After equalizing the received symbol using $\hat{S}(i,m) = \frac{Y(i,m)}{\hat{H}_0(\rho_m)}$, Channel estimation and symbol estimation steps are applied repeatedly until possible convergence.

At low SNR, the performance of the algorithms degrades as the symbol by symbol detection has poor performance.

4.7.3 Decision Directed with Time Truncation (DD-TT) Algorithm

In this section a novel semi blind channel estimation and tracking algorithm is proposed for highly dynamic V2V environments.

In our algorithm, we use decision directed channel estimation to get an initial estimate then a simple time truncation is done. A detailed explanation of the algorithm is listed as follows.

1. We will start with the LS estimate $\hat{H}_{LS}$ as an initial estimate then channel equalization of the first data symbol is done by the LS initial estimate as follows

$$\hat{S}_t(k) = \frac{Y_t(k)}{\hat{H}_{t-1}(k)} \tag{4.51}$$

where $\hat{S}_t(k)$ is the equalized symbol at subcarrier k and time t, $Y_t(k)$ is the received symbol at subcarrier k and time t and $\hat{H}_{t-1}(k)$ is the channel estimate of the previous symbol.

2. A further modification is done using the demodulated data to get a more accurate channel estimates as shown below

$$H_{init,\, t}(k) = \frac{Y_t(k)}{\hat{X}_t(k)} \tag{4.52}$$

where $\hat{X}_t(k)$ is the demodulated symbol from $\hat{S}_t(k)$.

3. A much better estimate is obtained using the time truncation technique.

The coefficients of each subcarrier is modified according to equation (15) then truncating the channel in the time domain by removing any existing taps rather than the first 8 taps defined by the V2V channel model, so any extra taps must equal to zero. And then iterate starting from equation (15) until there is no change in the subcarriers' coefficients. Each iteration requires only one 64-point FFT and one 64-point IFFT. And since the channel estimates converges most of the time after only 2 iterations, Thus time truncation technique has low complexity.

$$\hat{\mathbf{H}}_{\mathbf{DD-TT}} = \arg \min_{\lambda_m[\hat{H}^J(k)]^{1/J}} ||H_{init,\,t} - \lambda_m[\hat{H}^J(k)]^{1/J}|| \qquad (4.53)$$

where $\hat{H}(k) = Y_t(k)$. Then the pilots majority rule is used to ensure correct channel polarity as in the FA-TT algorithm.

This algorithm is simple to implement and its performance is independent of neither the packet size nor the vehicle velocity and on the other hand it gives the best performance reached compared to previous channel estimation techniques used for V2V communications.

The reason behind this performance gain is noise cancellation by calculating the initial channel estimate using the demodulated data and also exploiting the pilots' information to determine the channel polarity with a great degree of confidence using the majority rule. Moreover, exploiting the number of taps of the V2V channel model gives the high performance boost to the algorithm. Besides the fact that estimating the channel taps depends only on the channel of the previous symbol as well as the current one makes the algorithm able to track the channel fast variations.

4.7.4 Performance Comparison

CDP and iterative-DD algorithms didn't meet the expected performance levels and fails to track the channel responce even at low mobility enviroments.

Decision Directed Time Truncation achieve a very good performance with low computational complexity for highly mobile environments and large packet sizes.
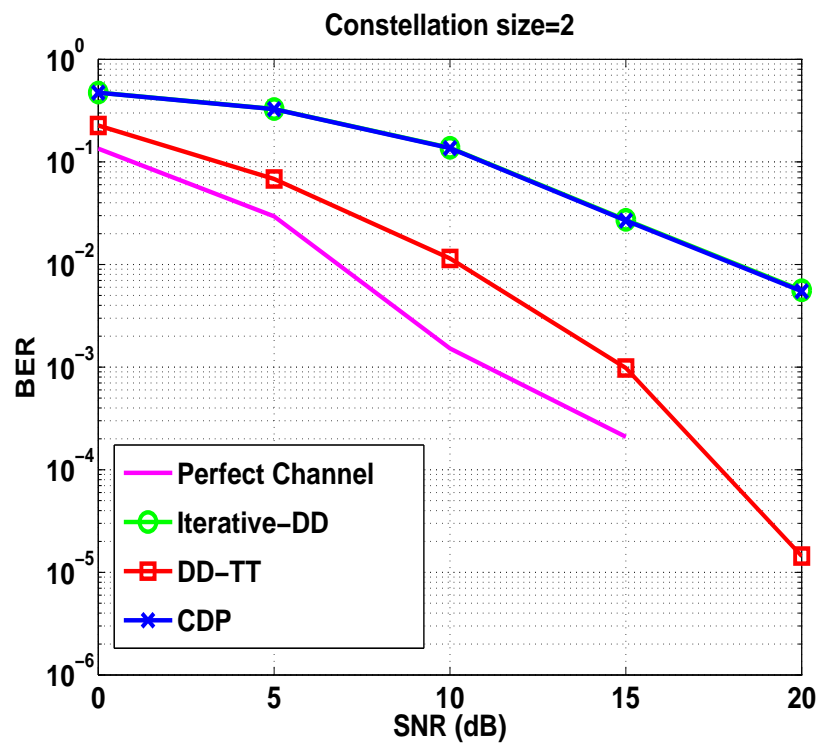

FIGURE 4.23: BPSK Bit Error Rate, maximum doppler=200Hz and 50 OFDM symbol per packet.

FIGURE 4.24: BPSK Bit Error Rate, maximum doppler=500Hz and 50 OFDM symbol per packet.

FIGURE 4.25: BPSK Bit Error Rate, maximum doppler=1000Hz and 100 OFDM symbol per packet.

FIGURE 4.26: BPSK Bit Error Rate, maximum doppler=1000Hz and 200 OFDM symbol per packet.

FIGURE 4.27: BPSK Bit Error Rate, maximum doppler=500Hz and 100 OFDM symbol per packet.

4.8 Discussion

Thus, the proposed schemes achieve BER performance beyond the reach of the conventional schemes. In summary, simulation results showed that the proposed scheme reduces the BER at all modulation schemes for all channel models and all packet sizes. Fig. 4.27 through Fig. 4.31 show the BER performance of the different channel estimation and tracking algorithms. We can clearly see some significant performance gains of the proposed DD-TT and MD-TT as compared to the STA algorithm of [5].
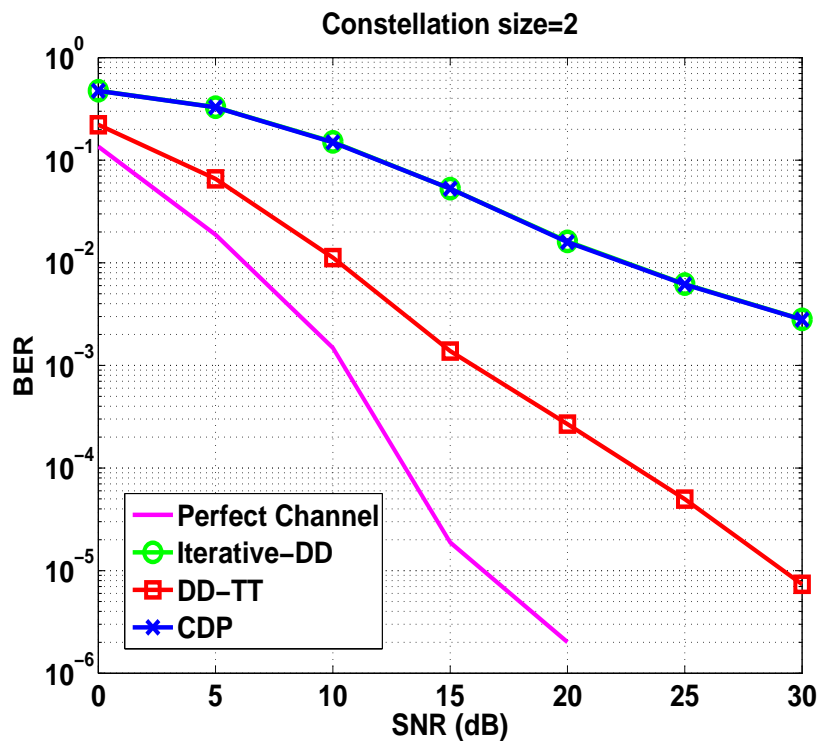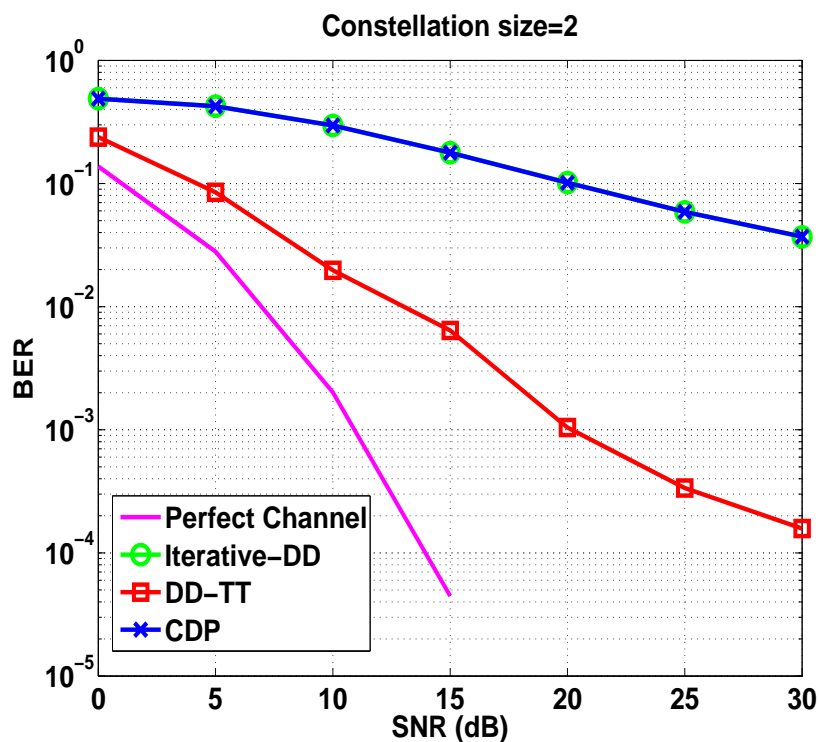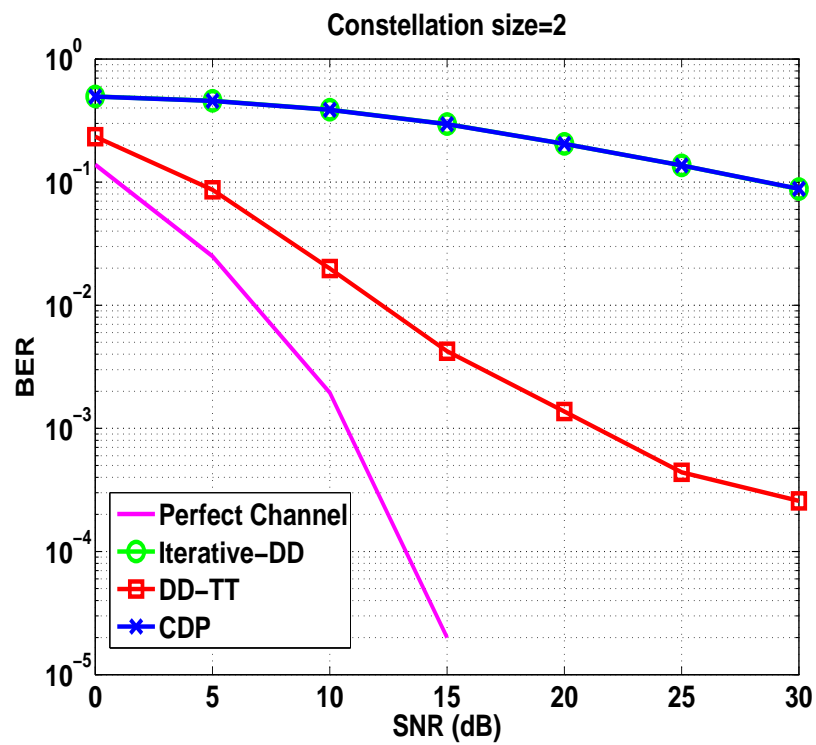
FIGURE 4.28: BPSK Bit Error Rate, maximum doppler=1000Hz and 100 OFDM symbol per packet.

FIGURE 4.29: BPSK Bit Error Rate, maximum doppler=1000Hz and 200 OFDM symbol per packet.
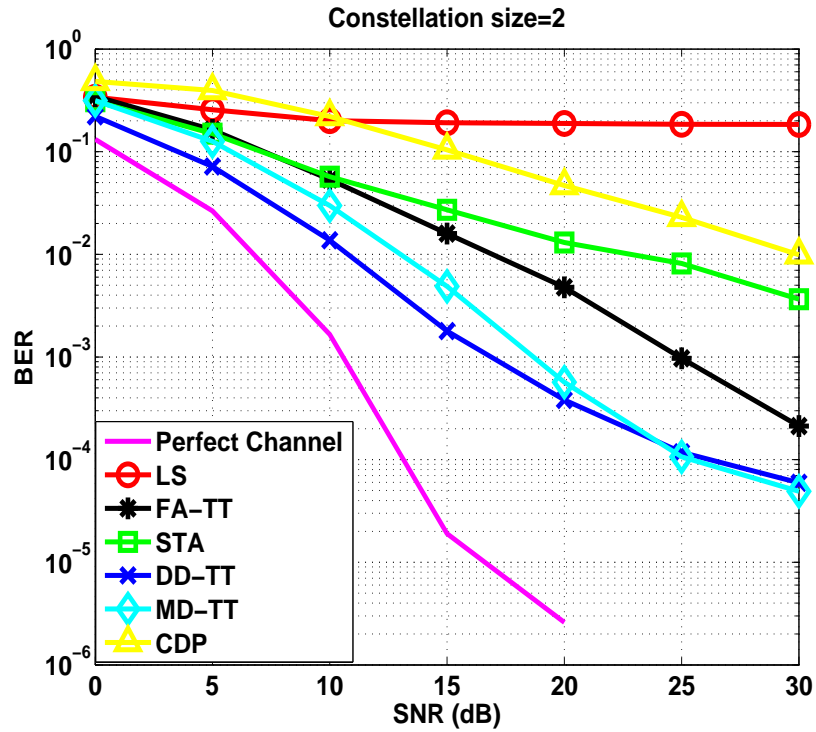
FIGURE 4.30: QPSK Bit Error Rate, maximum doppler=1000Hz and 50 OFDM symbol per packet.
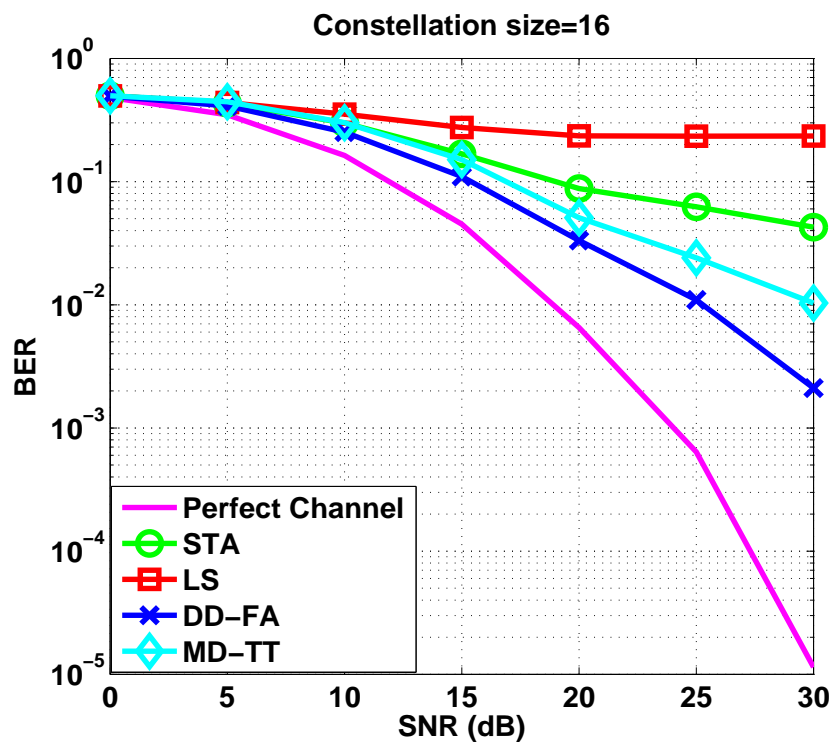
FIGURE 4.31: 16QAM Bit Error Rate, maximum doppler=1000Hz and 25 OFDM symbol per packet.
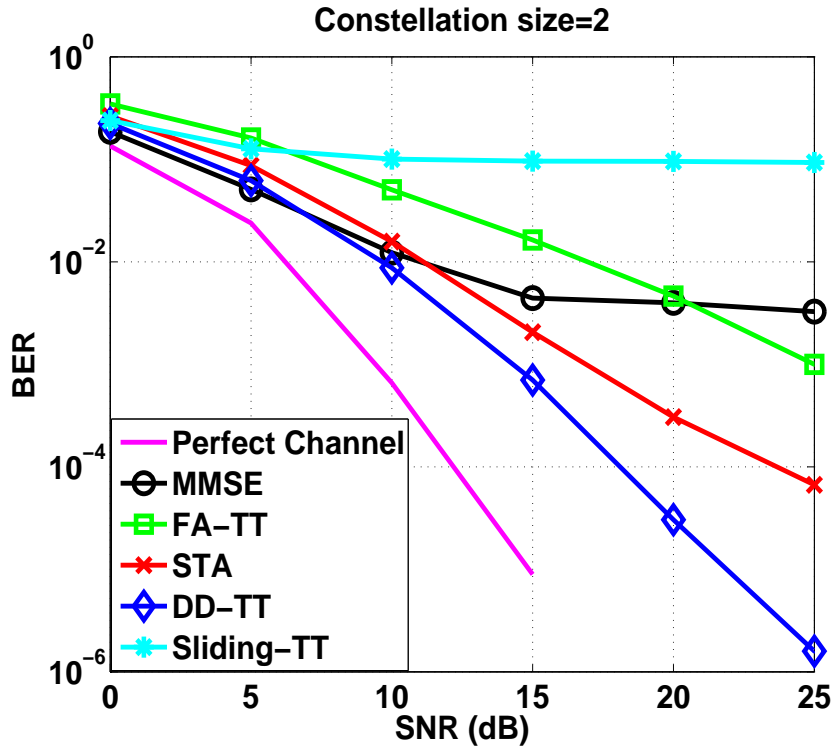
FIGURE 4.32: BPSK Bit Error Rate, maximum doppler=200Hz and 50 OFDM symbol per packet.

FA-TT, MD-TT and DD-TT are the most powerful algorithms for three reasons and Fig.4.32 to Fig. 4.35 show the following:

First, the three algorithms achieve very high performance for low mobile environments as well as fast varying channels.

Second, the algorithms withstand different packet sizes and achieve a very good performance even for large packet sizes.

Last, both the MD-TT and DD-TT have low computational complexity even for higher constellation sizes and that is why these two algorithms are more suitable for implementation than the FA-TT algorithm.

FIGURE 4.33: BPSK Bit Error Rate, maximum doppler=500Hz and 50 OFDM symbol per packet.
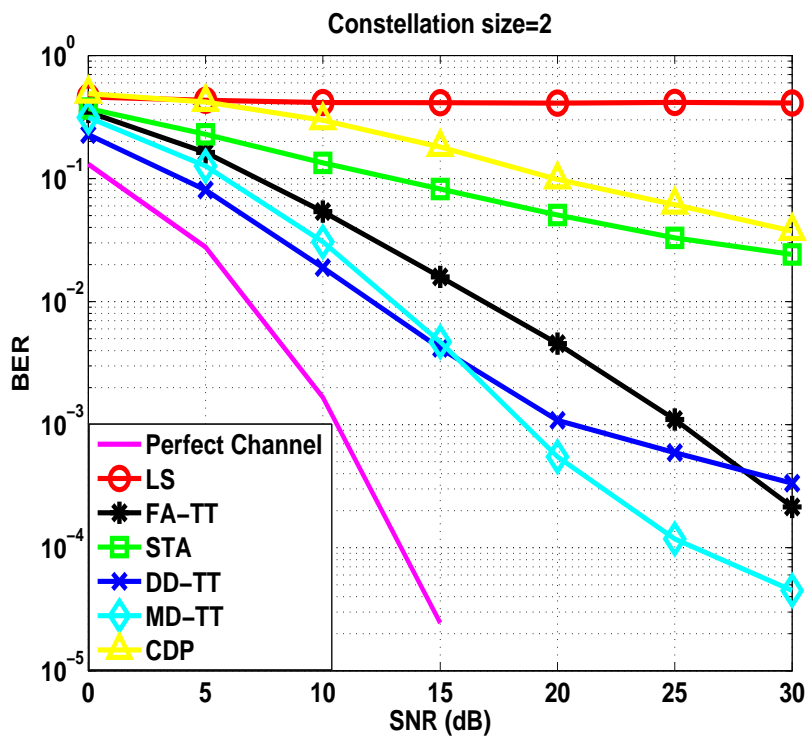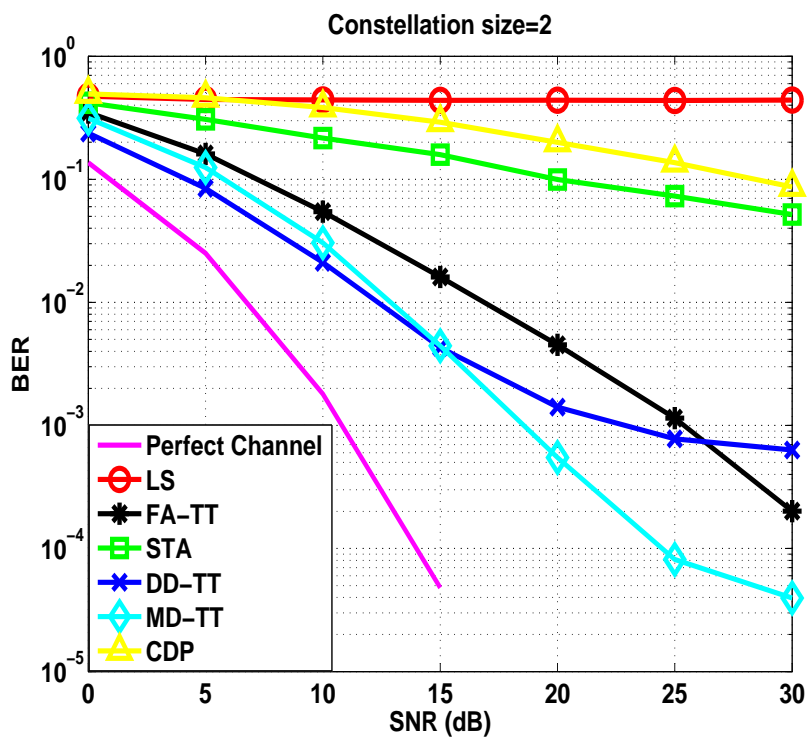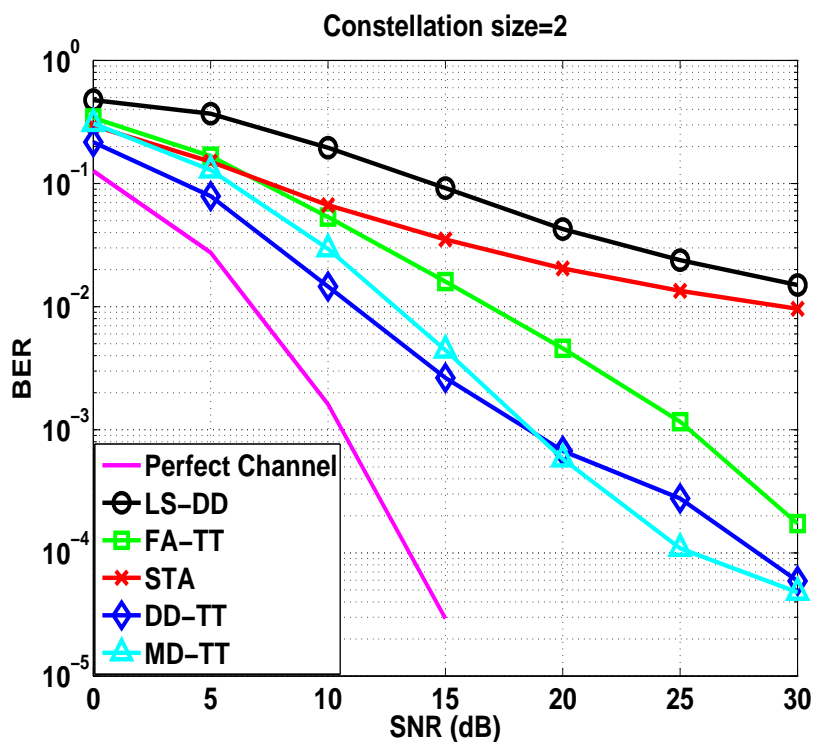

FIGURE 4.34: BPSK Bit Error Rate, maximum doppler=1000Hz and 50 OFDM symbol per packet.
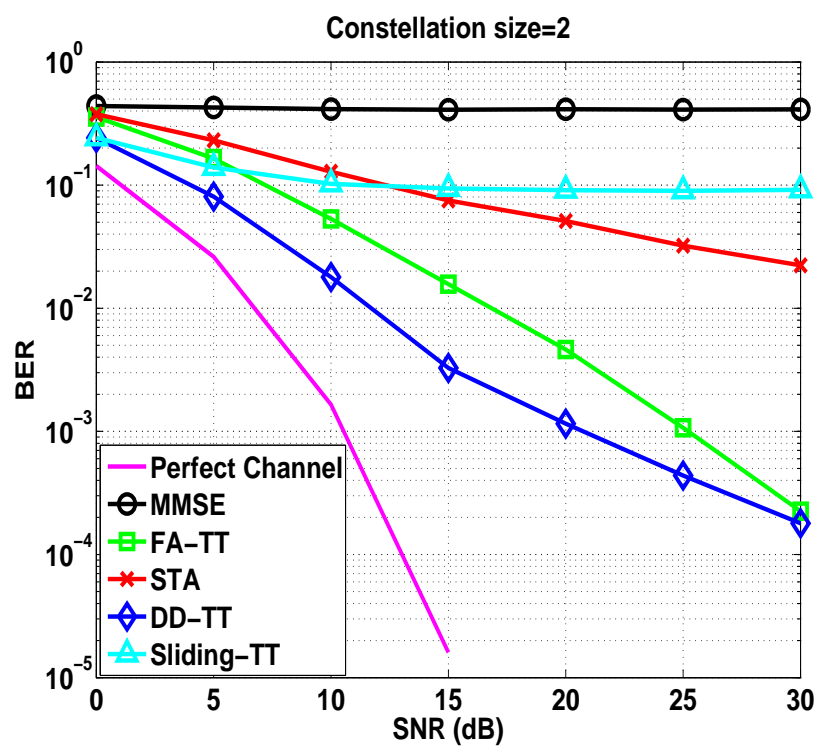
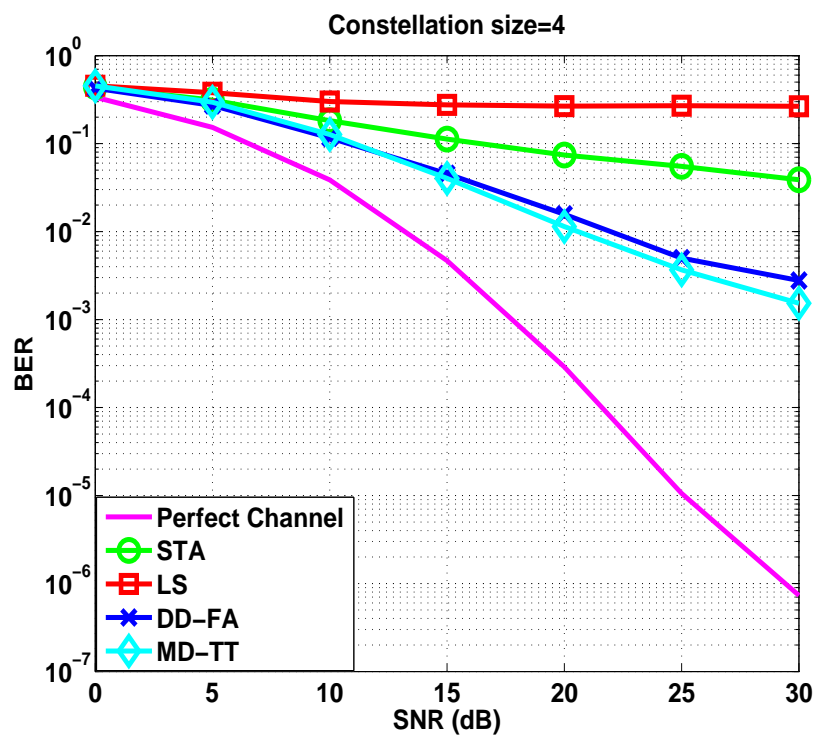FIGURE 4.35: BPSK Bit Error Rate, maximum doppler=1000Hz and 100 OFDM symbol per packet.
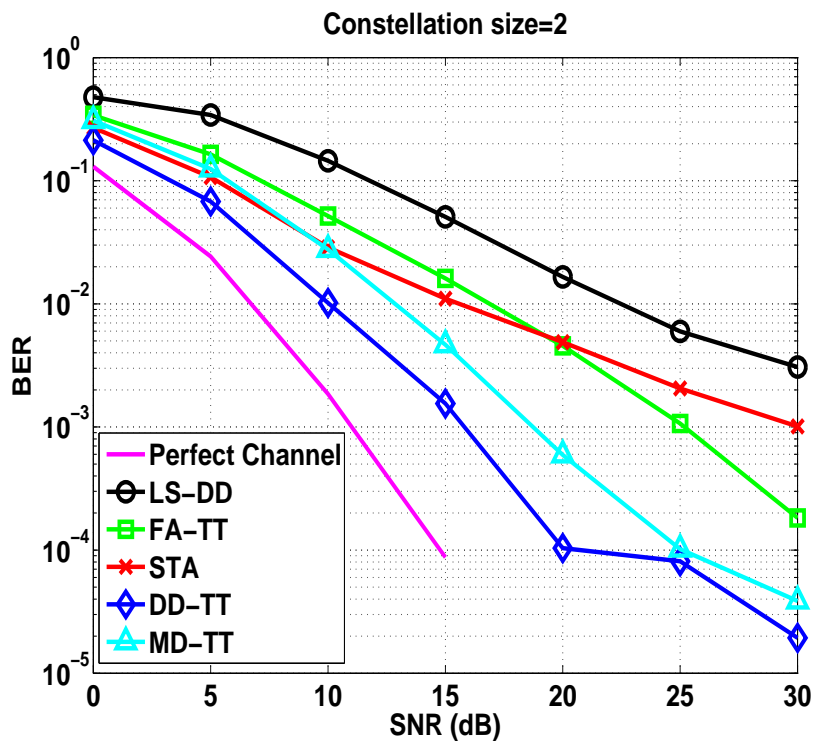
Chapter 5

Conclusion and Future Work

5.1 Conclusion

In this Thesis, we have presented several channel estimation and tracking algorithms for the V2V channels. A finite alphabet with time truncation (FA-TT), a decision-directed with time truncation (DD-TT) and minimum distance with time truncation (MD-TT) channel estimators were proposed for the 5.9 GHz DSRC receiver. The algorithms achieve very high performance for low mobile environments as well as fast varying channels even for large packet sizes. The designed channel estimators were compared to conventional and other previously proposed channel estimators using simulation under V2V channel models. The receivers with DD-TT and MD-TT estimators improved BER performance in all modulation schemes, namely BPSK, QPSK and 16-QAM. The receiver with the designed estimators achieved performances that were not at all possible with conventional estimators. The proposed DD-TT and MD-TT designs were shown to be very effective and practical for WAVE applications, since it is simple, compliant with the IEEE802.11p standard and did not require extensive hardware complexity.

5.2 Future Work

Although the proposed receiver design achieved a higher performance than any other conventional receiver but a lot more is expected by applying different estimation techniques for the IEEE 802.11p standard and compare their performance in the V2V environment.

Besides, a hardware implementation of DD-TT and MD-TT schemes are required to illustrate their implementation feasibility.

Bibliography

[1] Rohde and Schwarz. Wlan 802.11p measurements for vehicle to vehicle (v2v) dsrc application note, 2009. URL http://www.rohde-schwarz.de/file/1MA152_2e.pdf.

[2] Liuqing Yang and Fei-Yue Wang. Driving into intelligent spaces with pervasive communications. *Intelligent Systems, IEEE*, 22(1):12–15, Jan 2007. ISSN 1541-1672. doi: 10.1109/MIS.2007.8.

[3] Fengzhong Qu, Fei-Yue Wang, and Liuqing Yang. Intelligent transportation spaces: vehicles, traffic, communications, and beyond. *Communications Magazine, IEEE*, 48(11):136–142, November 2010. ISSN 0163-6804. doi: 10.1109/MCOM.2010.5621980.

[4] J.A Fernandez, K. Borries, Lin Cheng, B.V.K.V. Kumar, D.D. Stancil, and Fan Bai. Performance of the 802.11p physical layer in vehicle-to-vehicle environments. *Vehicular Technology, IEEE Transactions on*, 61(1):3–14, Jan 2012. ISSN 0018-9545. doi: 10.1109/TVT.2011.2164428.

[5] J.A. Fernandez, D.D. Stancil, and Fan Bai. Dynamic channel equalization for ieee 802.11p waveforms in the vehicle-to-vehicle channel. In *Communication, Control, and Computing (Allerton), 2010 48th Annual Allerton Conference on*, pages 542–551, Sept 2010. doi: 10.1109/ALLERTON.2010.5706954.

[6] H. Abdulhamid, E. Abdel-Raheem, and K.E. Tepe. Channel estimation for 5.9 ghz dedicated shortrange communications receiver in wireless access vehicular environments. *Communications, IET*, 1(6):1274–1279, Dec 2007. ISSN 1751-8628. doi: 10.1049/iet-com:20060639.

[7] A Bourdoux, H. Cappelle, and A Dejonghe. Channel tracking for fast time-varying channels in ieee802.11p systems. In *Global Telecommunications Conference (GLOBECOM 2011), 2011 IEEE*, pages 1–6, Dec 2011. doi: 10.1109/GLOCOM.2011.6134024.

[8] Zijun Zhao, Xiang Cheng, Miaowen Wen, BingLi Jiao, and Cheng-Xiang Wang. Channel estimation schemes for ieee 802.11p standard. *Intelligent Transportation Systems Magazine, IEEE*, 5(4):38–49, winter 2013. ISSN 1939-1390. doi: 10.1109/MITS.2013.2270032.

[9] M. Belotserkovsky. An equalizer initialization algorithm for ieee802.11a and hiperlan/2 receivers. *Consumer Electronics, IEEE Transactions on*, 48(4):1051–1055, Nov 2002. ISSN 0098-3063. doi: 10.1109/TCE.2003.1196438.

[10] T. Kella. Decision-directed channel estimation for supporting higher terminal velocities in ofdm based wlans. In *Global Telecommunications Conference, 2003. GLOBECOM '03. IEEE*, volume 3, pages 1306–1310 vol.3, Dec 2003. doi: 10.1109/GLOCOM.2003.1258449.

[11] Yong-Hua Cheng, Yi-Hung Lu, and Chia-Ling Liu. Adaptive channel equalizer for wireless access in vehicular environments. In *ITS Telecommunications Proceedings, 2006 6th International Conference on*, pages 1102–1105, June 2006. doi: 10.1109/ITST.2006.288780.

[12] Youwei Zhang, Ian L. Tan, Carl Chun, Ken Laberteaux, and Ahmad Bahai. A differential ofdm approach to coherence time mitigation in dsrc. In *VANET '08 Proceedings of the fifth ACM international workshop on VehiculAr Inter-NETworking*, pages 1102–1105, September 2008. doi: http://doi.acm.org/10.1145/1410043.1410045.

[13] Ieee standard for information technology– local and metropolitan area networks– specific requirements– part 11: Wireless lan medium access control (mac) and physical layer (phy) specifications amendment 6: Wireless access in vehicular environments. *IEEE Std 802.11p-2010 (Amendment to IEEE Std 802.11-2007 as amended by IEEE Std 802.11k-2008, IEEE Std 802.11r-2008, IEEE Std 802.11y-2008, IEEE Std 802.11n-2009, and IEEE Std 802.11w-2009)*, pages 1–51, July 2010. doi: 10.1109/IEEESTD.2010.5514475.

[14] Supplement to ieee standard for information technology - telecommunications and information exchange between systems - local and metropolitan area networks - specific requirements. part 11: Wireless lan medium access control (mac) and physical layer (phy) specifications: High-speed physical layer in the 5 ghz band. *IEEE Std 802.11a-1999*, pages i–, 1999. doi: 10.1109/IEEESTD.1999.90606.

[15] J.A.C. Bingham. Multicarrier modulation for data transmission: an idea whose time has come. *Communications Magazine, IEEE*, 28(5):5–14, May 1990. ISSN 0163-6804. doi: 10.1109/35.54342.

[16] G. Acosta-Marum and M.-A. Ingram. Six time- and frequency- selective empirical channel models for vehicular wireless lans. *Vehicular Technology Magazine, IEEE*, 2(4):4–11, Dec 2007. ISSN 1556-6072. doi: 10.1109/MVT.2008.917435.

[17] Gerges Dib. *Vehicle-to-vehicle channel simulation in a network simulator*. PhD thesis, Carnegie Mellon University, 2009.

[18] Tao Jiang, Hsiao-Hwa Chen, Hsiao-Chun Wu, and Youwen Yi. Channel modeling and inter-carrier interference analysis for v2v communication systems in frequency-dispersive channels. *Mobile Networks and Applications*, 15(1):4–12, 2010.

[19] A.F. Molisch, F. Tufvesson, J. Karedal, and C.F. Mecklenbrauker. A survey on vehicle-to-vehicle propagation channels. *Wireless Communications, IEEE*, 16(6): 12–22, December 2009. ISSN 1536-1284. doi: 10.1109/MWC.2009.5361174.

[20] Jeongwook Seo, Kyungwon Park, Wongi Jeon, J. Kwak, and Dong Ku Kim. Performance evaluation of v2x communications in practical small-scale fading models. In *Personal, Indoor and Mobile Radio Communications, 2009 IEEE 20th International Symposium on*, pages 2434–2438, Sept 2009. doi: 10.1109/PIMRC.2009.5450041.

[21] G. Acosta-Marum and M.-A. Ingram. Six time- and frequency- selective empirical channel models for vehicular wireless lans. *Vehicular Technology Magazine, IEEE*, 2(4):4–11, Dec 2007. ISSN 1556-6072. doi: 10.1109/MVT.2008.917435.

[22] Guillermo Acosta-Marum. Measurement, modeling, and ofdm synchronization for the wideband mobile-to-mobile channel. 2007.

[23] Mr ANIL KUMAR PATTANAYAK. Channel estimation in ofdm systems, 2007.

[24] Cheng-Xiang Wang, Xiang Cheng, and D.I. Laurenson. Vehicle-to-vehicle channel modeling and measurements: recent advances and future challenges. *Communications Magazine, IEEE*, 47(11):96–103, November 2009. ISSN 0163-6804. doi: 10.1109/MCOM.2009.5307472.

[25] Xiang Cheng, Cheng-Xiang Wang, D.I. Laurenson, S. Salous, and A.V. Vasilakos. An adaptive geometry-based stochastic model for non-isotropic mimo mobile-to-mobile channels. *Wireless Communications, IEEE Transactions on*, 8(9):4824–4835, September 2009. ISSN 1536-1276. doi: 10.1109/TWC.2009.081560.

[26] Xiang Cheng, Cheng-Xiang Wang, Haiming Wang, Xiqi Gao, Xiao-Hu You, Dongfeng Yuan, Bo Ai, Qiang Huo, Ling-Yang Song, and Bing-Li Jiao. Cooperative mimo channel modeling and multi-link spatial correlation properties. *Selected Areas in Communications, IEEE Journal on*, 30(2):388–396, February 2012. ISSN 0733-8716. doi: 10.1109/JSAC.2012.120218.

[27] Xiang Cheng, Cheng-Xiang Wang, Bo Ai, and H. Aggoune. Envelope level crossing rate and average fade duration of nonisotropic vehicle-to-vehicle ricean fading channels. *Intelligent Transportation Systems, IEEE Transactions on*, 15(1):62–72, Feb 2014. ISSN 1524-9050. doi: 10.1109/TITS.2013.2274618.

[28] Xiaohu Ge, Kun Huang, Cheng-Xiang Wang, Xuemin Hong, and Xi Yang. Capacity analysis of a multi-cell multi-antenna cooperative cellular network with co-channel interference. *Wireless Communications, IEEE Transactions on*, 10(10):3298–3309, October 2011. ISSN 1536-1276. doi: 10.1109/TWC.2011.11.101551.

[29] Cheng-Xiang Wang, Xuemin Hong, Xiaohu Ge, Xiang Cheng, Gong Zhang, and J. Thompson. Cooperative mimo channel models: A survey. *Communications Magazine, IEEE*, 48(2):80–87, February 2010. ISSN 0163-6804. doi: 10.1109/MCOM.2010.5402668.

[30] Xiang Cheng, Qi Yao, Cheng-Xiang Wang, Bo Ai, G.L. Stuber, Dongfeng Yuan, and Bing-Li Jiao. An improved parameter computation method for a mimo v2v rayleigh fading channel simulator under non-isotropic scattering environments. *Communications Letters, IEEE*, 17(2):265–268, February 2013. ISSN 1089-7798. doi: 10.1109/LCOMM.2013.011113.121535.

[31] Fengzhong Qu and Liuqing Yang. On the estimation of doubly-selective fading channels. *Wireless Communications, IEEE Transactions on*, 9(4):1261–1265, April 2010. ISSN 1536-1276. doi: 10.1109/TWC.2010.04.080631.

[32] I. Sen and D.W. Matolak. Vehicle-vehicle channel models for the 5-ghz band. *Intelligent Transportation Systems, IEEE Transactions on*, 9(2):235–245, June 2008. ISSN 1524-9050. doi: 10.1109/TITS.2008.922881.

[33] Xiang Cheng, Qi Yao, Miaowen Wen, Cheng-Xiang Wang, Ling-Yang Song, and Bing-Li Jiao. Wideband channel modeling and intercarrier interference cancellation for vehicle-to-vehicle communication systems. *Selected Areas in Communications, IEEE Journal on*, 31(9):434–448, September 2013. ISSN 0733-8716. doi: 10.1109/JSAC.2013.SUP.0513039.

[34] G. Acosta-Marum and M.-A. Ingram. Six time- and frequency- selective empirical channel models for vehicular wireless lans. *Vehicular Technology Magazine, IEEE*, 2(4):4–11, Dec 2007. ISSN 1556-6072. doi: 10.1109/MVT.2008.917435.

[35] Sang In Kim, Hyun Seo Oh, and Hyun Kyun Choi. Mid-amble aided ofdm performance analysis in high mobility vehicular channel. In *Intelligent Vehicles Symposium, 2008 IEEE*, pages 751–754, June 2008. doi: 10.1109/IVS.2008.4621156.

[36] Woong Cho, Sang In Kim, Hyun Kyun Choi, Hyun Seo Oh, and Dong Yong Kwak. Performance evaluation of v2v/v2i communications: The effect of midamble insertion. In *Wireless Communication, Vehicular Technology, Information Theory and Aerospace Electronic Systems Technology, 2009. Wireless VITAE 2009. 1st International Conference on*, pages 793–797, May 2009. doi: 10.1109/WIRELESSVITAE.2009.5172551.

[37] Chi-Sheng Lin, Che-Kang Sun, Jia-Chin Lin, and Bo-Chuan Chen. Performance evaluations of channel estimations in ieee 802.11p environments. In *Ultra Modern Telecommunications Workshops, 2009. ICUMT '09. International Conference on*, pages 1–5, Oct 2009. doi: 10.1109/ICUMT.2009.5345402.

[38] Chi-Sheng Lin and Jia-Chin Lin. Novel channel estimation techniques in ieee 802.11p environments. In *Vehicular Technology Conference (VTC 2010-Spring), 2010 IEEE 71st*, pages 1–5, May 2010. doi: 10.1109/VETECS.2010.5493969.

[39] J. Nuckelt, M. Schack, and T. Kurner. Performance evaluation of wiener filter designs for channel estimation in vehicular environments. In *Vehicular Technology Conference (VTC Fall), 2011 IEEE*, pages 1–5, Sept 2011. doi: 10.1109/VETECF.2011.6093050.

[40] T. Zemen, L. Bernado, N. Czink, and A.F. Molisch. Iterative time-variant channel estimation for 802.11p using generalized discrete prolate spheroidal sequences. *Vehicular Technology, IEEE Transactions on*, 61(3):1222–1233, March 2012. ISSN 0018-9545. doi: 10.1109/TVT.2012.2185526.

[41] J.A. Fernandez, K. Borries, Lin Cheng, B.V.K.V. Kumar, D.D. Stancil, and Fan Bai. Performance of the 802.11p physical layer in vehicle-to-vehicle environments. *Vehicular Technology, IEEE Transactions on*, 61(1):3–14, Jan 2012. ISSN 0018-9545. doi: 10.1109/TVT.2011.2164428.

[42] A. Bourdoux, H. Cappelle, and A. Dejonghe. Channel tracking for fast time-varying channels in ieee802.11p systems. In *Global Telecommunications Conference (GLOBECOM 2011), 2011 IEEE*, pages 1–6, Dec 2011. doi: 10.1109/GLOCOM.2011.6134024.

[43] Amr El-Keyi, Tamer ElBatt, Fan Bai, and Cem Saraydar. Mimo vanets: Research challenges and opportunities. In *Computing, Networking and Communications (ICNC), 2012 International Conference on*, pages 670–676. IEEE, 2012.

[44] Harb Abdulhamid, Kemal E Tepe, and Esam Abdel-Raheem. Performance of dsrc systems using conventional channel estimation at high velocities. *AEU-International Journal of Electronics and Communications*, 61(8):556–561, 2007.

[45] J. Yin, T. ElBatt, G. Yeung, B. Ryu, S. Habermas, H. Krishnan, and T. Talty. Performance evaluation of safety applications over dsrc vehicular ad hoc networks. In *VANET '04 Proceedings of the 1st ACM international workshop on Vehicular ad hoc networks*, pages 1–9, October 2004. doi: http://doi.acm.org/10.1145/1023875.1023877.

[46] S. Sibecas, C.A. Corral, S. Emami, and G. Stratis. On the suitability of 802.11a/ra for high-mobility dsrc. In *Vehicular Technology Conference, 2002. VTC Spring 2002. IEEE 55th*, volume 1, pages 229–234 vol.1, 2002. doi: 10.1109/VTC.2002.1002698.

[47] J.-J. van de Beek, O. Edfors, M. Sandell, S.K. Wilson, and P. Ola Borjesson. On channel estimation in ofdm systems. In *Vehicular Technology Conference, 1995 IEEE 45th*, volume 2, pages 815–819 vol.2, Jul 1995. doi: 10.1109/VETEC.1995.504981.

[48] Yushi Shen and Ed Martinez. Channel estimation in ofdm systems, 2006. URL http://www.freescale.com/files/dsp/doc/app_note/AN3059.pdf.

[49] Shengli Zhou and G.B. Giannakis. Finite-alphabet based channel estimation for ofdm and related multicarrier systems. *Communications, IEEE Transactions on*, 49(8):1402–1414, Aug 2001. ISSN 0090-6778. doi: 10.1109/26.939873.

[50] Meng-Han Hsieh and Che-Ho Wei. Channel estimation for ofdm systems based on comb-type pilot arrangement in frequency selective fading channels. *Consumer Electronics, IEEE Transactions on*, 44(1):217–225, Feb 1998. ISSN 0098-3063. doi: 10.1109/30.663750.

[51] Ye Li. Pilot-symbol-aided channel estimation for ofdm in wireless systems. *Vehicular Technology, IEEE Transactions on*, 49(4):1207–1215, Jul 2000. ISSN 0018-9545. doi: 10.1109/25.875230.

[52] S. Coleri, M. Ergen, A. Puri, and A. Bahai. Channel estimation techniques based on pilot arrangement in ofdm systems. *Broadcasting, IEEE Transactions on*, 48(3): 223–229, Sep 2002. ISSN 0018-9316. doi: 10.1109/TBC.2002.804034.

[53] S. Sibecas, C.A. Corral, S. Emami, G. Stratis, and G. Rasor. Pseudo-pilot ofdm scheme for 802.11a and r/a in dsrc applications. In *Vehicular Technology Conference, 2003. VTC 2003-Fall. 2003 IEEE 58th*, volume 2, pages 1234–1237 Vol.2, Oct 2003. doi: 10.1109/VETECF.2003.1285219.

[54] Zong-Sian Lin, Tze-Lun Hong, and Dah-Chung Chang. Design of an ofdm system with long frame by the decision-aided channel tracking technique. In *Electro/information Technology, 2006 IEEE International Conference on*, pages 330–333, May 2006. doi: 10.1109/EIT.2006.252179.

[55] S. Kalyani and K. Giridhar. Quantised decision based gradient descent algorithm for fast fading ofdm channels. In *Vehicular Technology Conference, 2004. VTC2004-Fall. 2004 IEEE 60th*, volume 1, pages 534–537 Vol. 1, Sept 2004. doi: 10.1109/VETECF.2004.1400064.

[56] R. Funada, H. Harada, and S. Shinoda. Performance improvement of decision-directed channel estimation for dpc-of/tdma in a fast fading environment. In *Vehicular Technology Conference, 2004. VTC2004-Fall. 2004 IEEE 60th*, volume 7, pages 5125–5129 Vol. 7, Sept 2004. doi: 10.1109/VETECF.2004.1405077.

[57] Hyung-Woo Kim, Chae-Hyun Lim, and Dong-Seong Han. Viterbi decoder aided equalization and sampling clock tracking for ofdm wlan. In *Vehicular Technology Conference, 2004. VTC2004-Fall. 2004 IEEE 60th*, volume 5, pages 3738–3742 Vol. 5, Sept 2004. doi: 10.1109/VETECF.2004.1404763.

[58] Qingsheng Yuan and Chen He. Channel estimation and equalization for ofdm system with fast fading channels. In *Signal Processing, 2004. Proceedings. ICSP '04. 2004 7th International Conference on*, volume 2, pages 1662–1665 vol.2, Aug 2004. doi: 10.1109/ICOSP.2004.1441652.

[59] T. Kella. Decision-directed channel estimation for supporting higher terminal velocities in ofdm based wlans. In *Global Telecommunications Conference, 2003. GLOBECOM '03. IEEE*, volume 3, pages 1306–1310 vol.3, Dec 2003. doi: 10.1109/GLOCOM.2003.1258449.

[60] R. Funada, H. Harada, Y. Kamio, S. Shinoda, and M. Fujise. A high-mobility packet transmission scheme based on conventional standardized ofdm formats. In *Vehicular Technology Conference, 2002. Proceedings. VTC 2002-Fall. 2002 IEEE 56th*, volume 1, pages 204–208 vol.1, 2002. doi: 10.1109/VETECF.2002.1040333.